

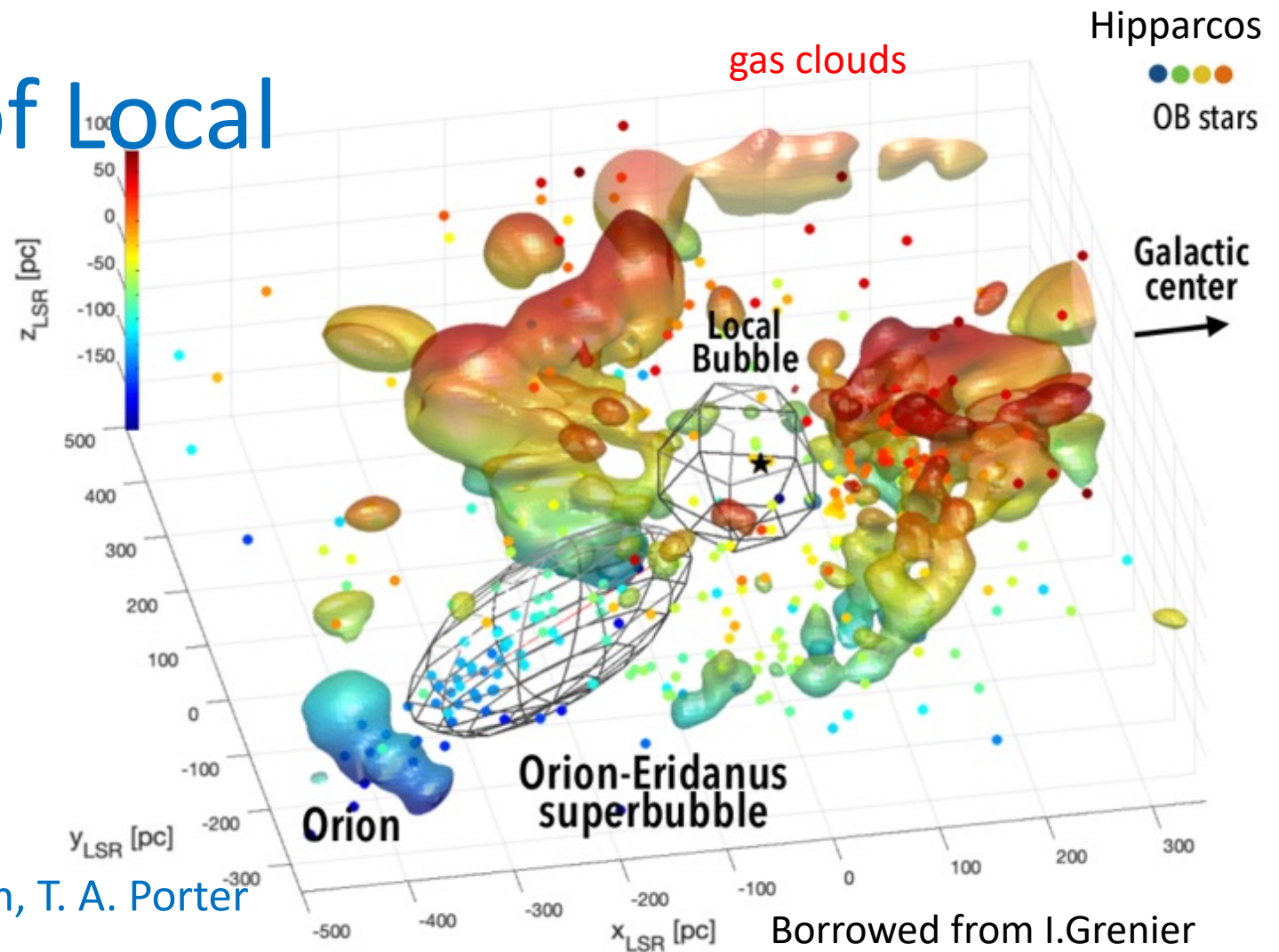
Spectral Signatures of Local Cosmic Ray Sources

Igor V Moskalenko / Stanford

with

A. C. Cummings, B. C. Heikkila, G. Johannesson, T. A. Porter

M. J. Boschini, S. Della Torre, M. Gervasi, D. Grandi, G. Jóhannesson, G. La Vacca, N. Masi, S. Pensotti, T.A. Porter, L. Quadrani, P.G. Rancoita, D. Rozza, M. Tacconi



Cosmic ray conference

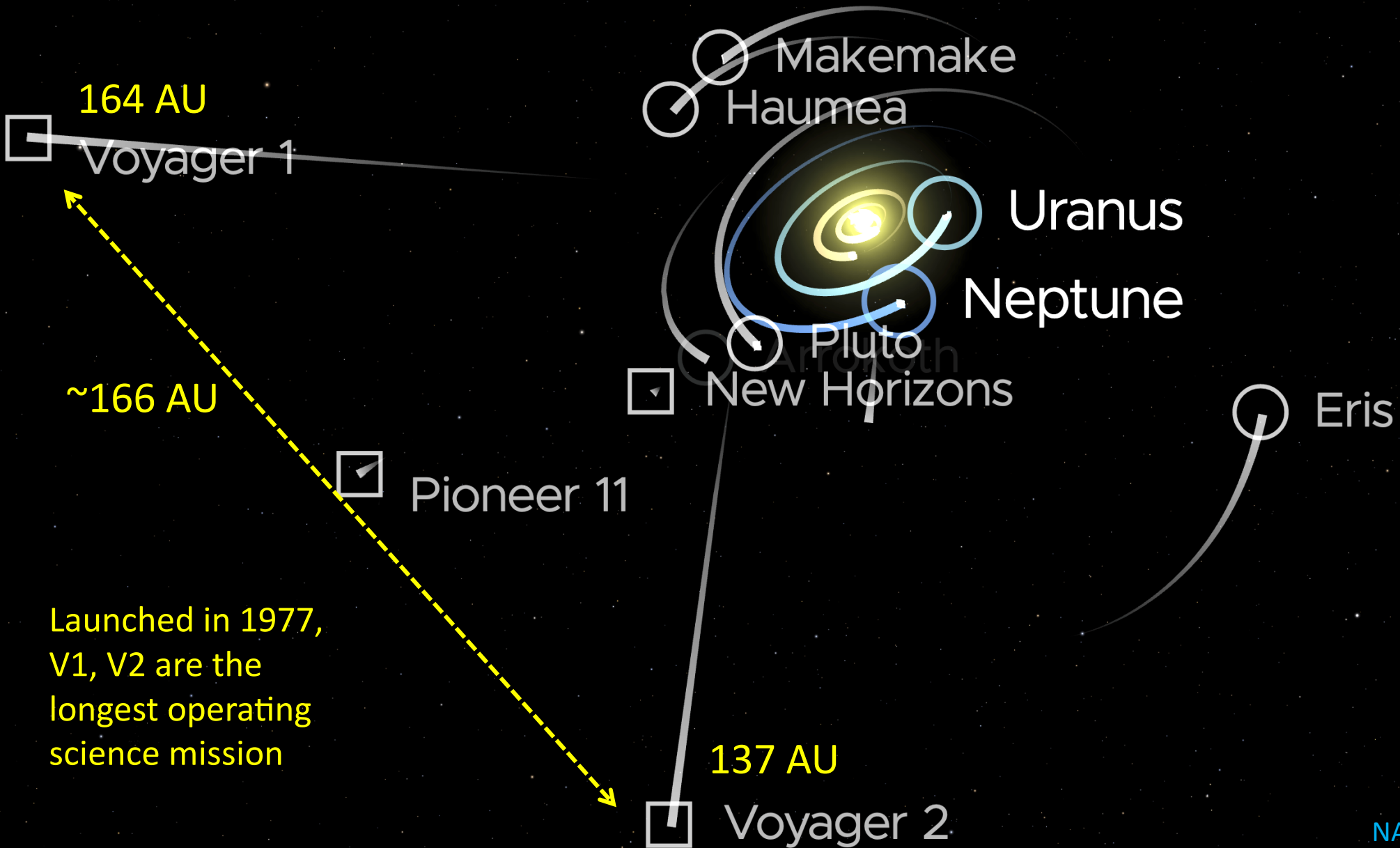


Voyager 1: Deuterium & Boron excesses



Current position

☐ Pioneer 10
137 AU



164 AU

Voyager 1

~166 AU

☐ Pioneer 11

☐ New Horizons

137 AU

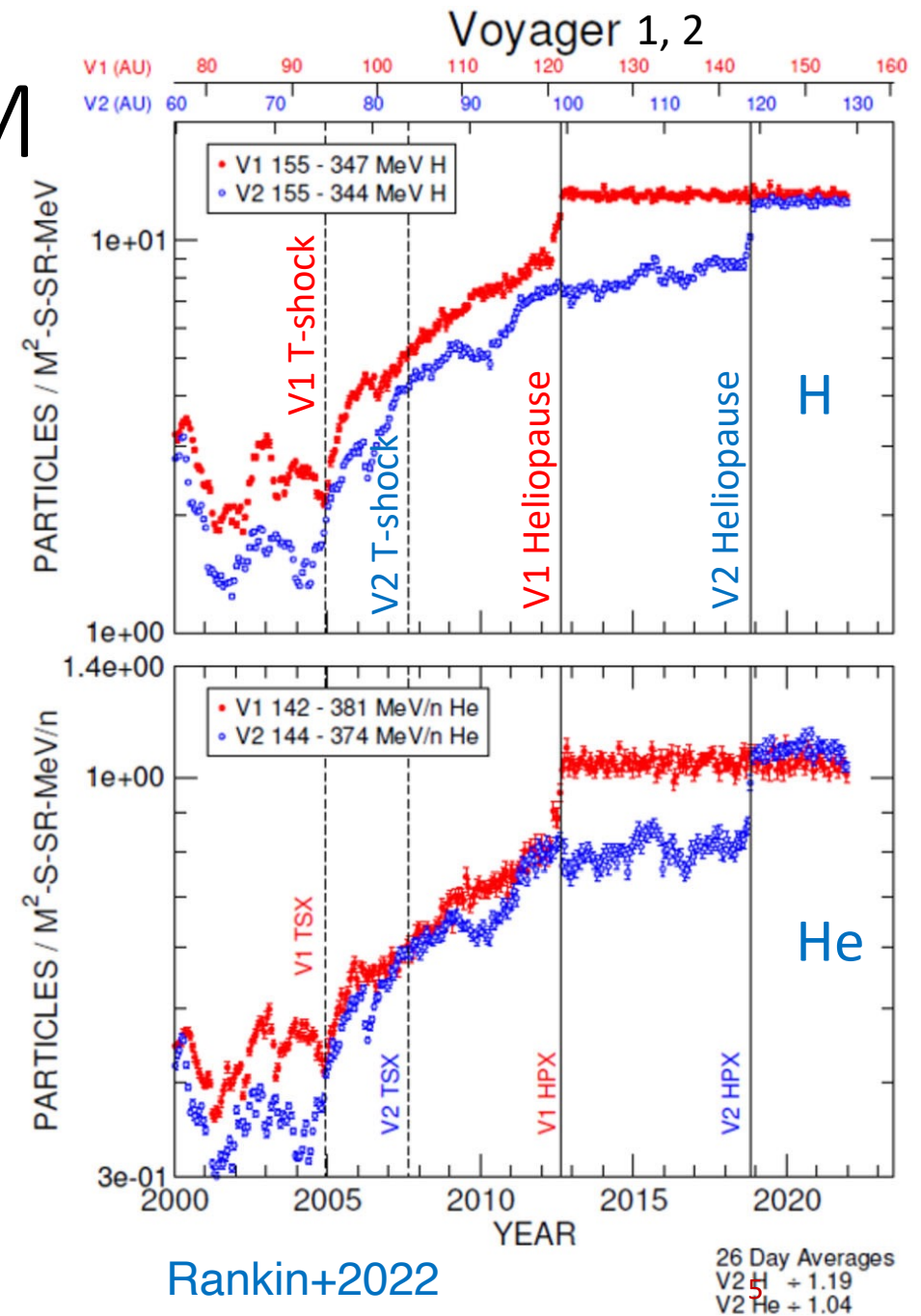
☐ Voyager 2

Eris

Launched in 1977,
V1, V2 are the
longest operating
science mission

Cosmic rays in the very local ISM

- 26-day averages of GCR Hydrogen and Helium measured by **Voyager 1** and **Voyager 2** as a function of time and radial distance in the Heliosheath and VLISM
- After the Heliopause crossing, the cosmic ray flux (H, He) remains constant





GALACTIC COSMIC RAYS IN THE LOCAL INTERSTELLAR MEDIUM: *VOYAGER 1* OBSERVATIONS AND MODEL RESULTS

A. C. CUMMINGS¹, E. C. STONE¹, B. C. HEIKKILA², N. LAL², W. R. WEBBER³, G. JÓHANNESSEN⁴,
I. V. MOSKALENKO⁵, E. ORLANDO⁵, AND T. A. PORTER⁵

¹California Institute of Technology, Pasadena, CA 91125, USA

²Goddard Space Flight Center, Greenbelt, MD 20771, USA

³New Mexico State University, Las Cruces, NM 88003, USA

⁴University of Iceland, Reykjavik, Iceland

⁵HEPL and KIPAC, Stanford University, Stanford, CA 94305, USA

Received 2016 March 29; revised 2016 April 21; accepted 2016 April 22; published 2016 October 21

- **2016 paper:** Data collected 2012/342 through 2015/181 ~ 2.5 years
- **2024 paper:** Updated data set 1/1/2013 through 12/31/2021 = 9 years

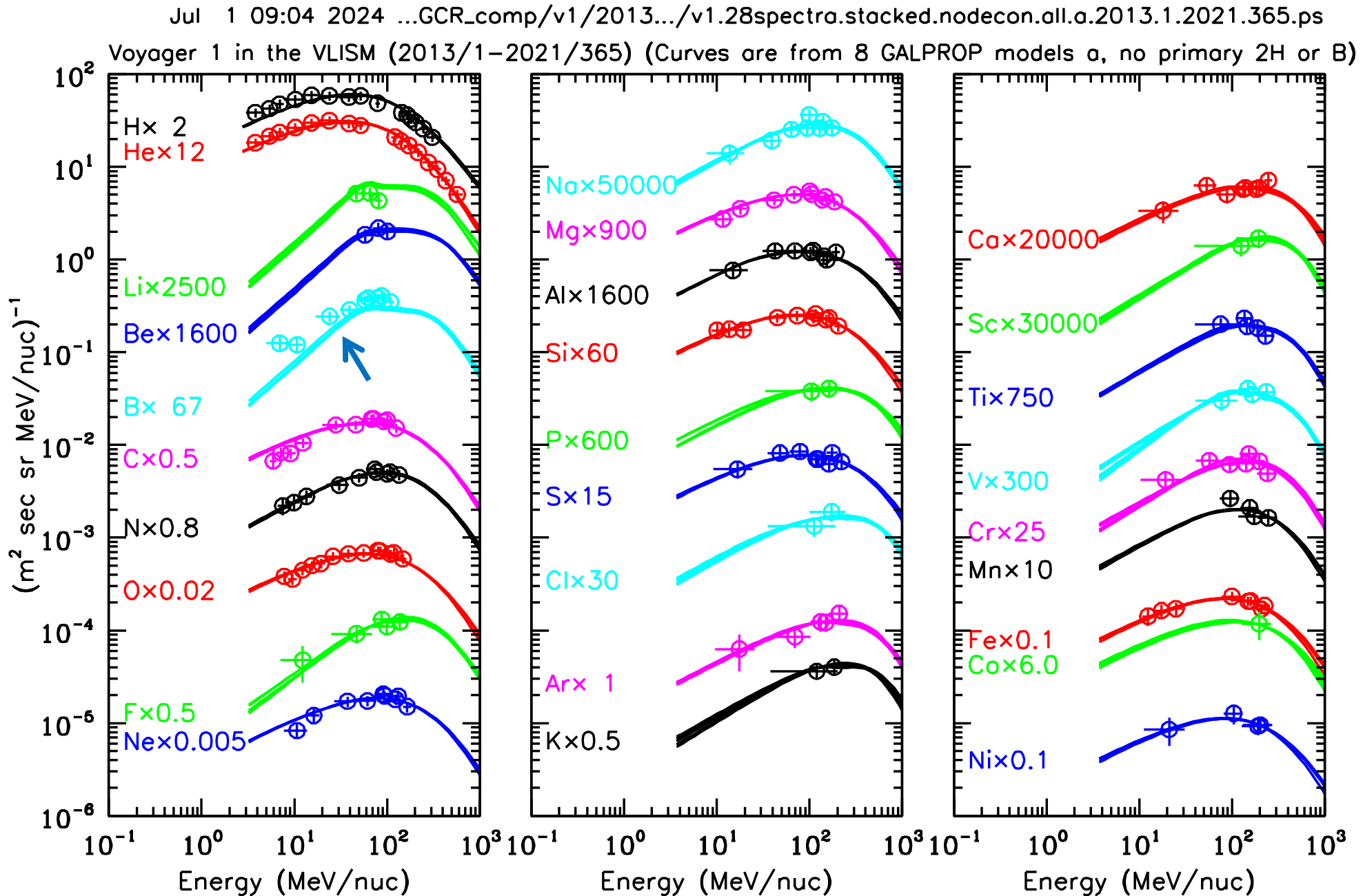
Submitted, 2024:

**Voyager 1 Observations of Galactic Cosmic Ray Isotopes in the Very Local Interstellar Medium:
Evidence for Primary ²H and B**

A. C. CUMMINGS,¹ I. V. MOSKALENKO,^{2,3} B. C. HEIKKILA,⁴ G. JÓHANNESSEN,⁵ AND T. A. PORTER^{2,3}

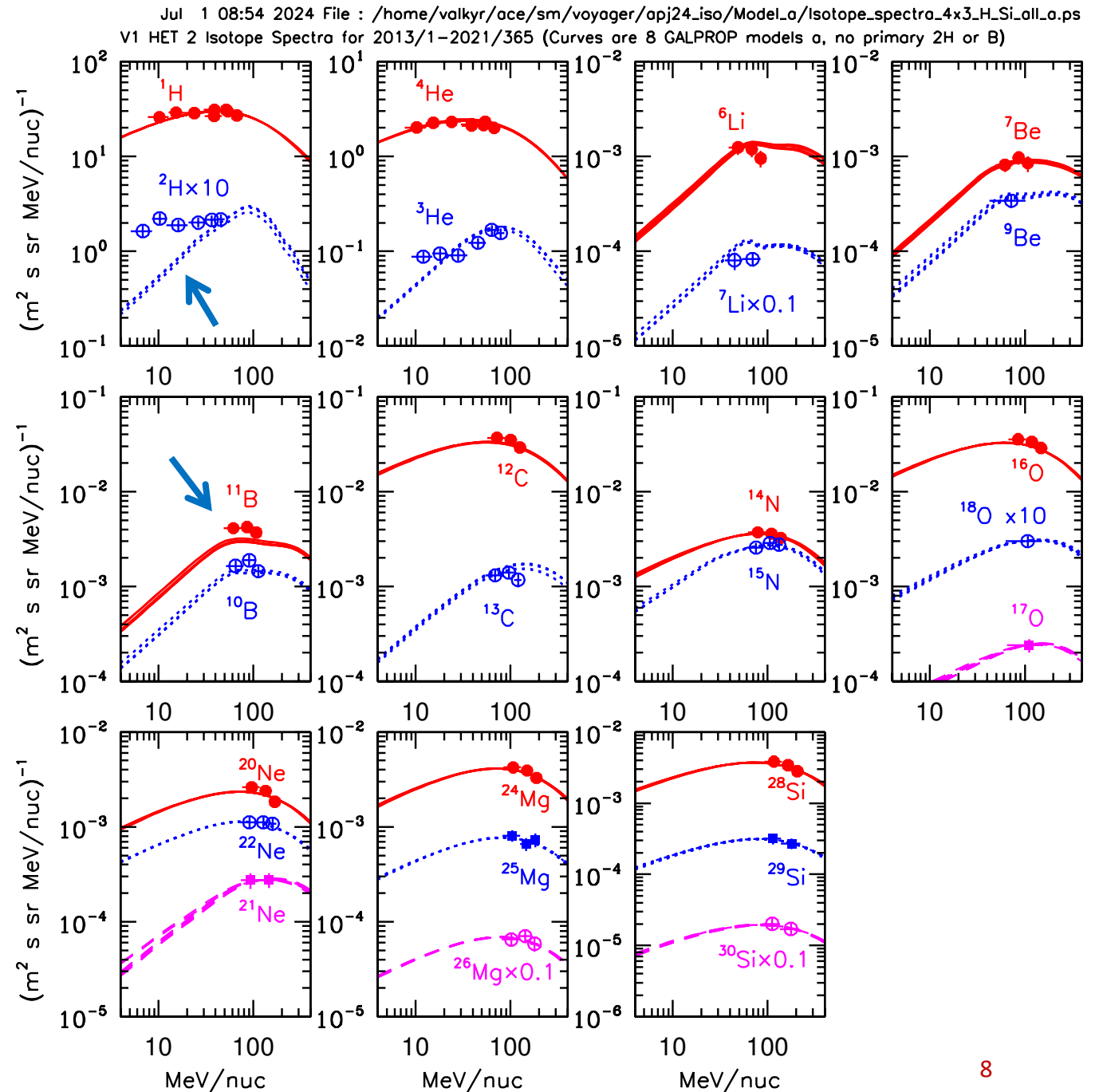
Elemental spectra

- Agree well with standard plain diffusion GALPROP models, except for the Boron excess at $\sim 3\sigma$ - 6σ level
- Details of the 8 GALPROP models are in the following slides
- All model spectra are consistent



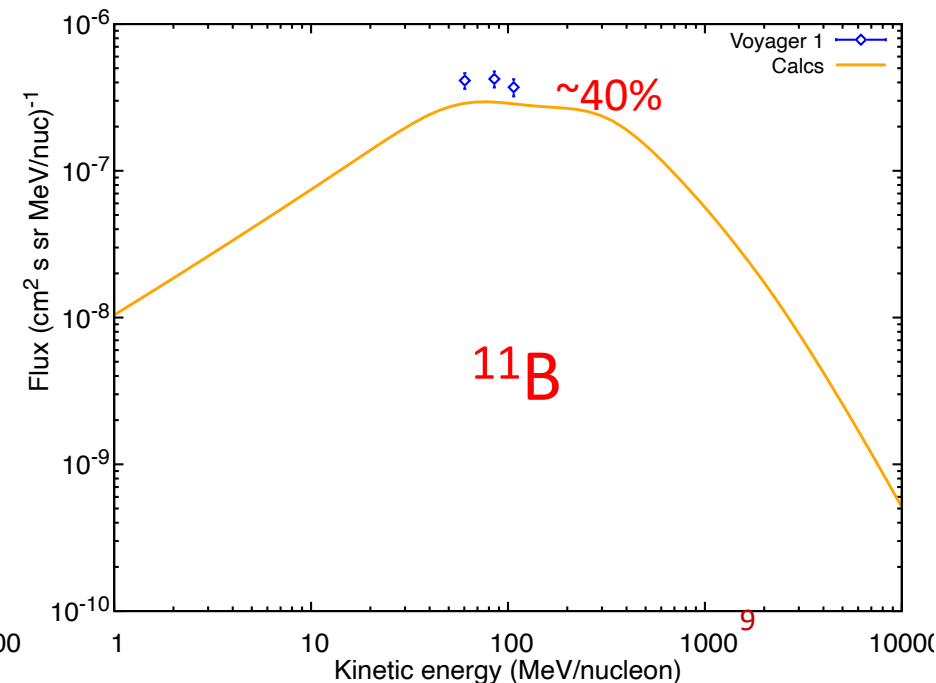
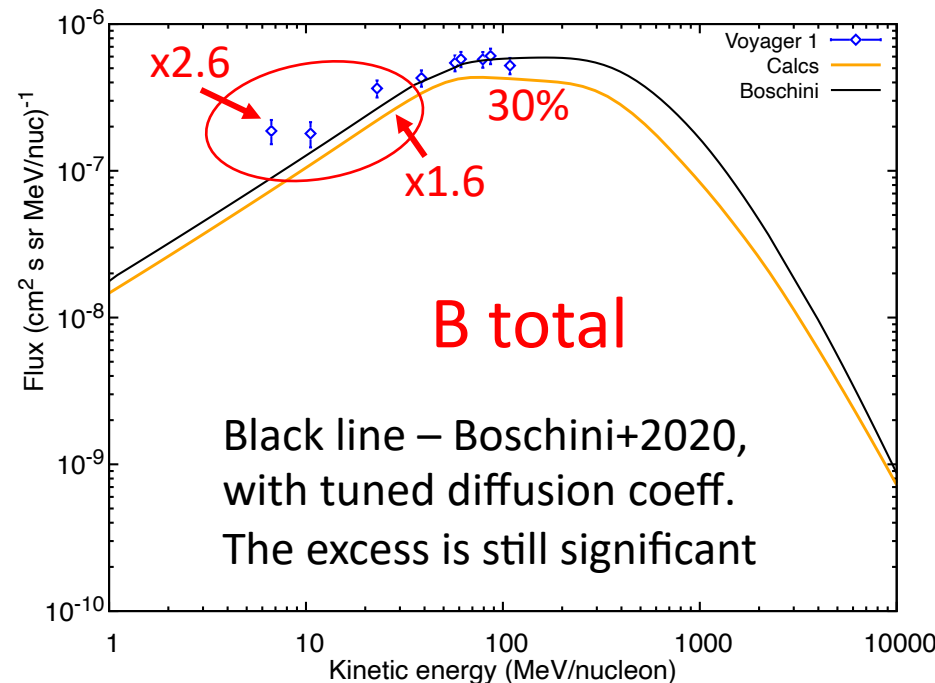
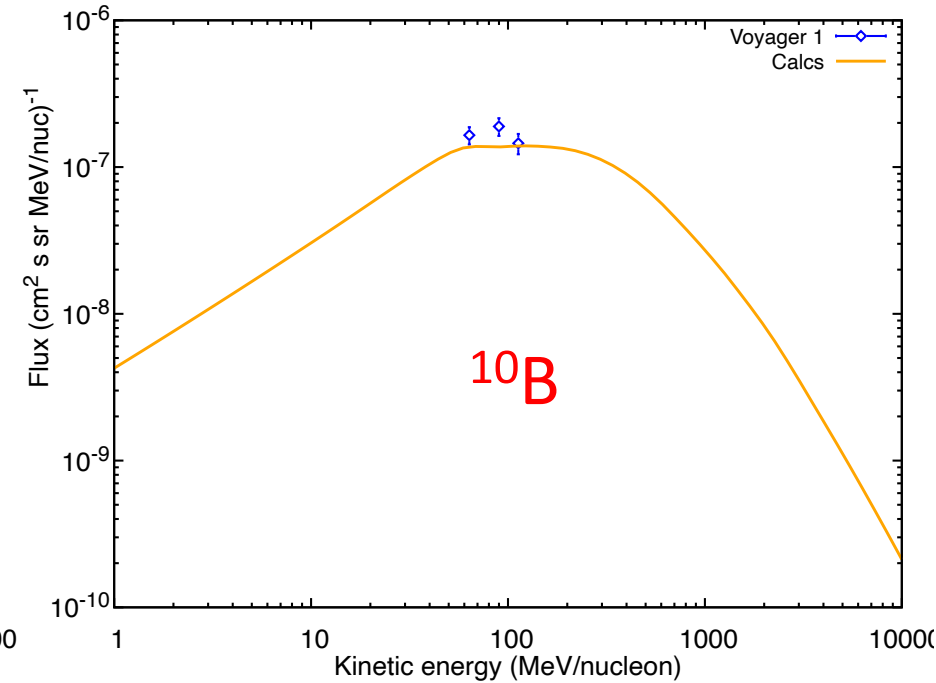
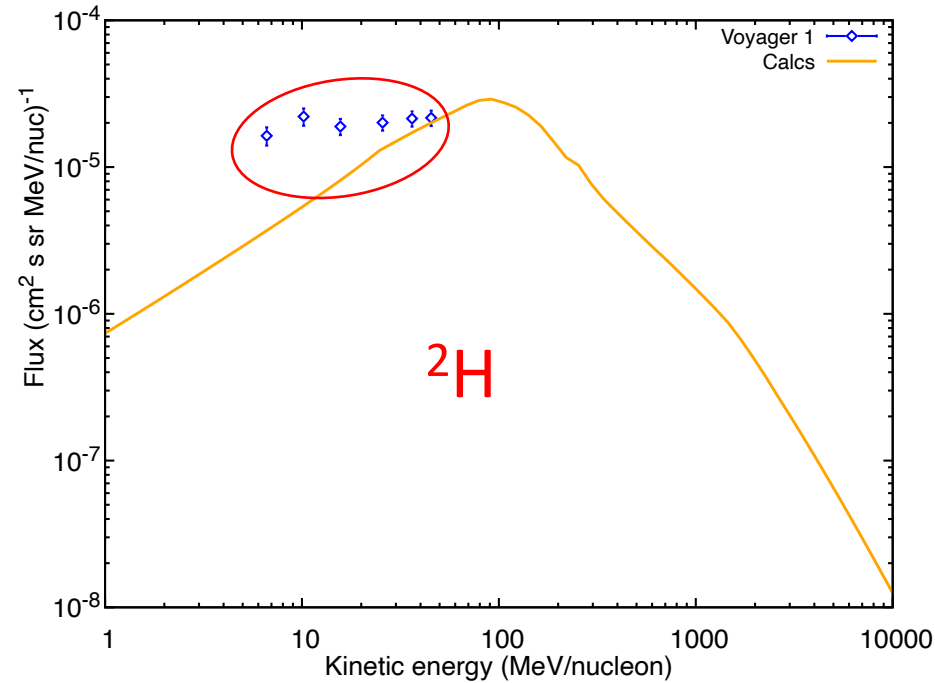
Isotopic spectra

- Although **8 GALPROP models** have different propagation parameters derived independently, the isotopic spectra are all consistent
- Source abundances (conventional):
 ${}^2\text{H}$, ${}^3\text{He}$, Li, Be, B = 0
- The agreement is good, except for ${}^2\text{H}$ and ${}^{11}\text{B}+{}^{10}\text{B}$
- **Boron:** Tried many options including increased weight of B data points (up to x100) – did not work well (e.g. C becomes crazy)
- Origin of ${}^2\text{H}$ and B excess – see following slides



Voyager 1 2H and B

- **Brown line** – model calculations with **zero source abundances**
- Excess in ^2H is very significant
- Excess in ^{11}B is $\sim 40\%$
- Excess in B_{tot} above 30 MeV/n is $\sim 30\%$
- Significant excesses **x1.6** and **x2.6** at 23 MeV/n and at 7 MeV/n



GALPROP models

- Use only Voyager 1 data – there is no modulation
- Tuned to match the local interstellar spectra (LIS, Boschini+2020) at higher energies
- Ionization energy losses at low energies are fast, reacceleration and convection are slow processes => Plain Diffusion Model – fewer parameters
- Single injection index for all species
- 8 models to cover available options in cross sections = 2 options for isotopic production cross sections × 4 options for total inelastic cross sections
- Worked hard to update the cross section parameterizations (see following slides) – this improvement gave us more confidence, but did not eliminate the ^2H and B excesses
- Source distribution: pulsar distribution by Lorimer+2006
- CO, H I, H II gas – standard distributions
- $X_{\text{CO}}(R) = 10^{19.6+0.066R} \text{ mol. cm}^{-2}/(\text{K km s}^{-1})$

Hypotheses of the origin of ^2H & B excesses

- i. Accuracy of isotopic production and fragmentation Xsections
- ii. Instrumental: production of ^2H & B in the window material
- iii. Primary ^2H & B components at low energies

Total inelastic cross sections

Existing data cover the energy range of interest: ~ 10 MeV/n – 100 MeV/n – removes the guesswork

Parameterizations:

$p+A$, $\alpha+A$

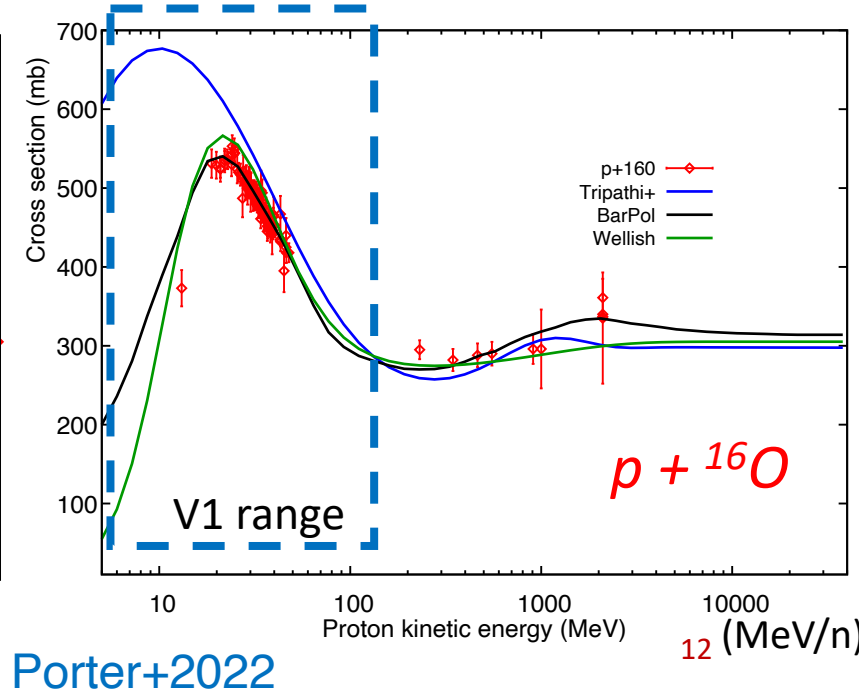
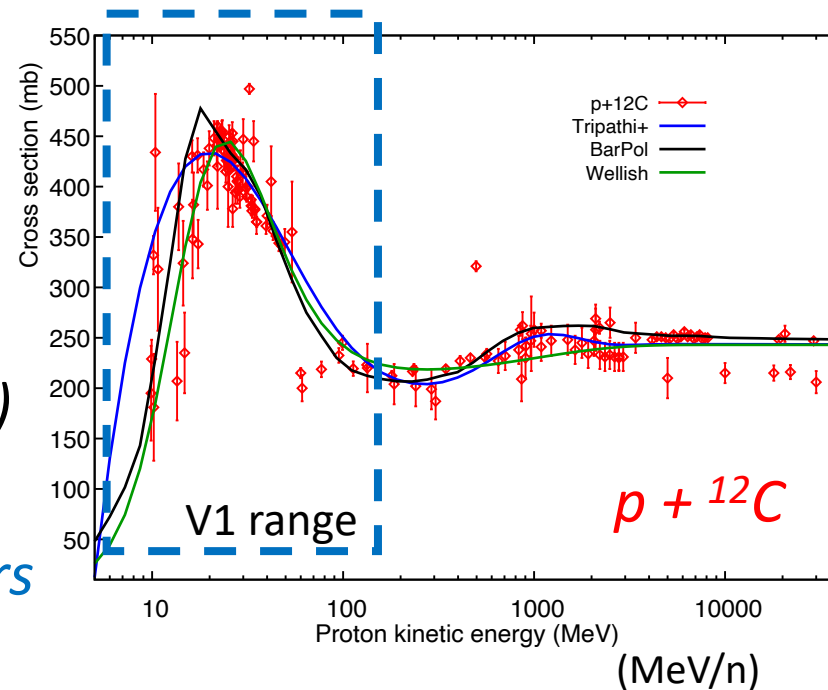
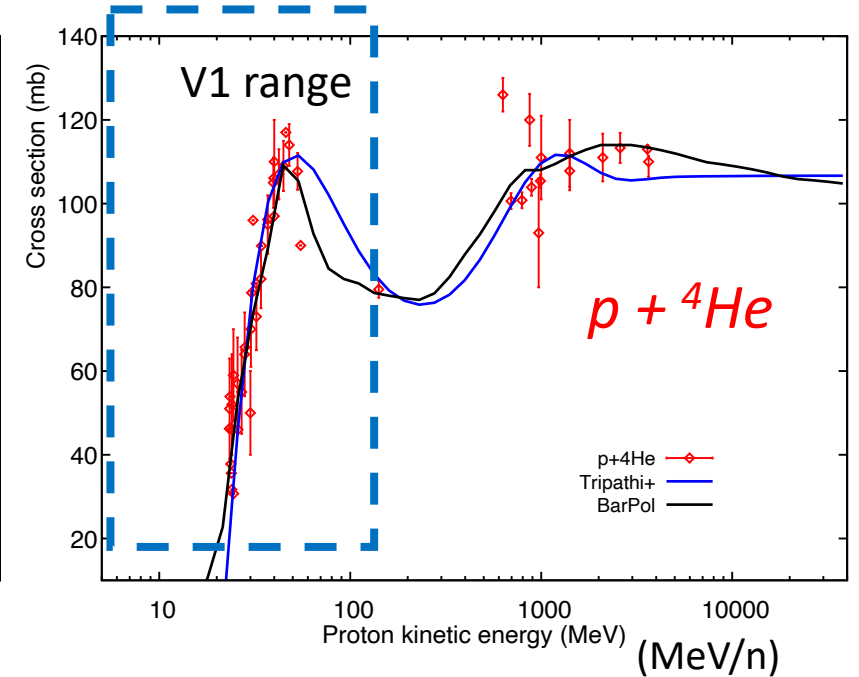
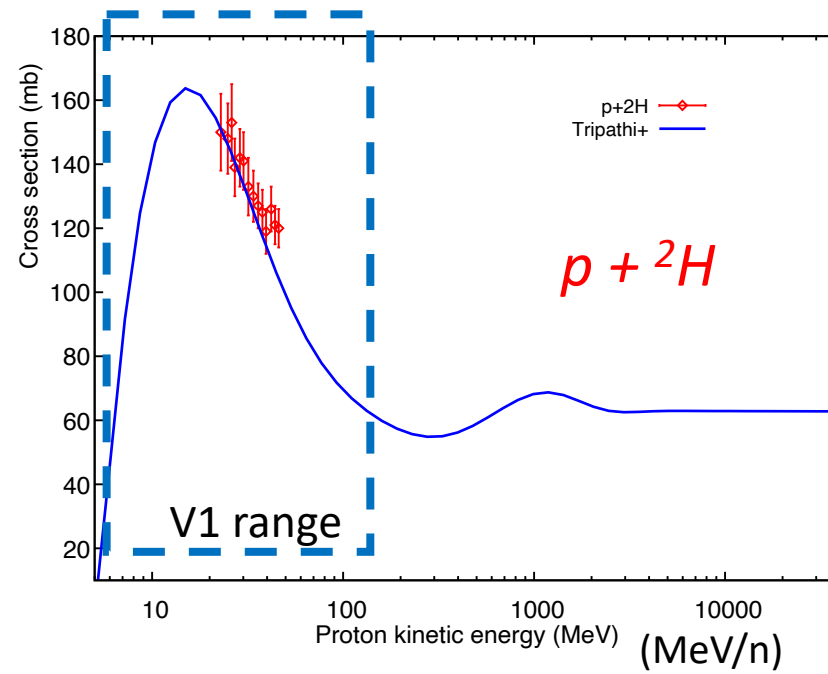
- *Tripathi+*

- *Barashenkov & Polansky*

$p+A$

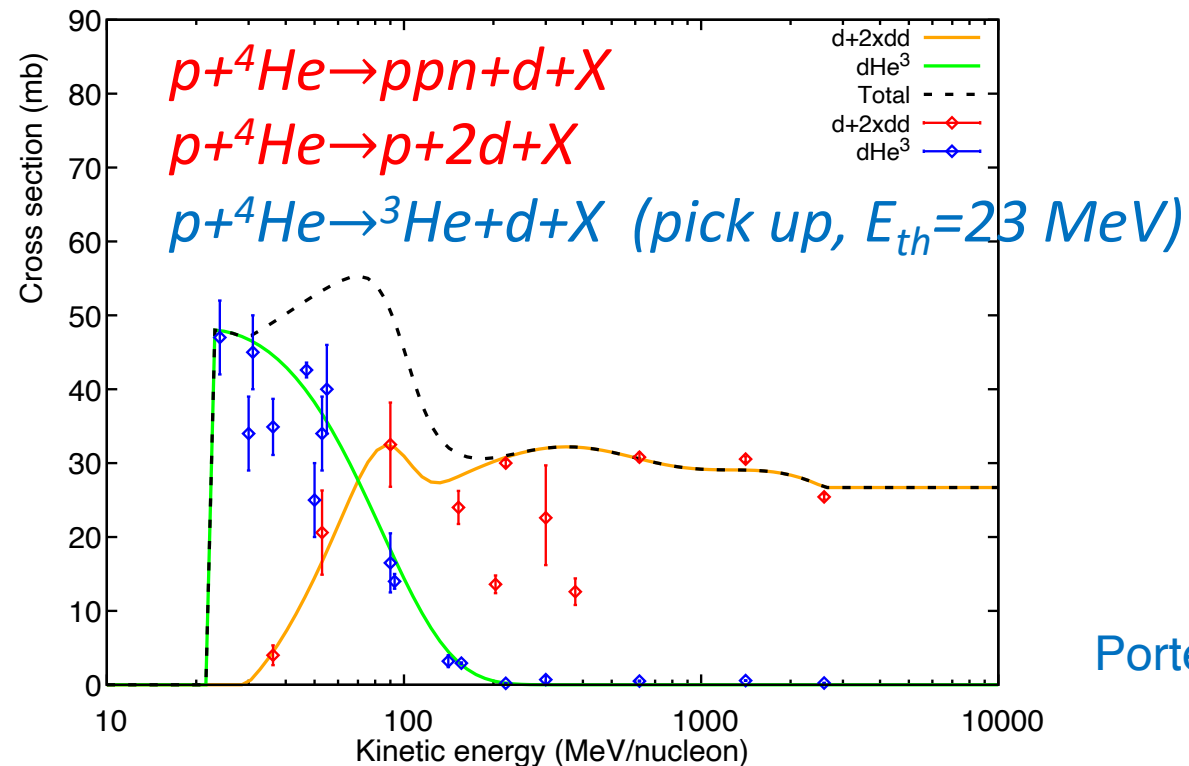
- *Wellisch & Axen 1996 (corr'd)*

Use their combinations to cover all projectile+target pairs



Deuteron production cross sections (GALPROP v57)

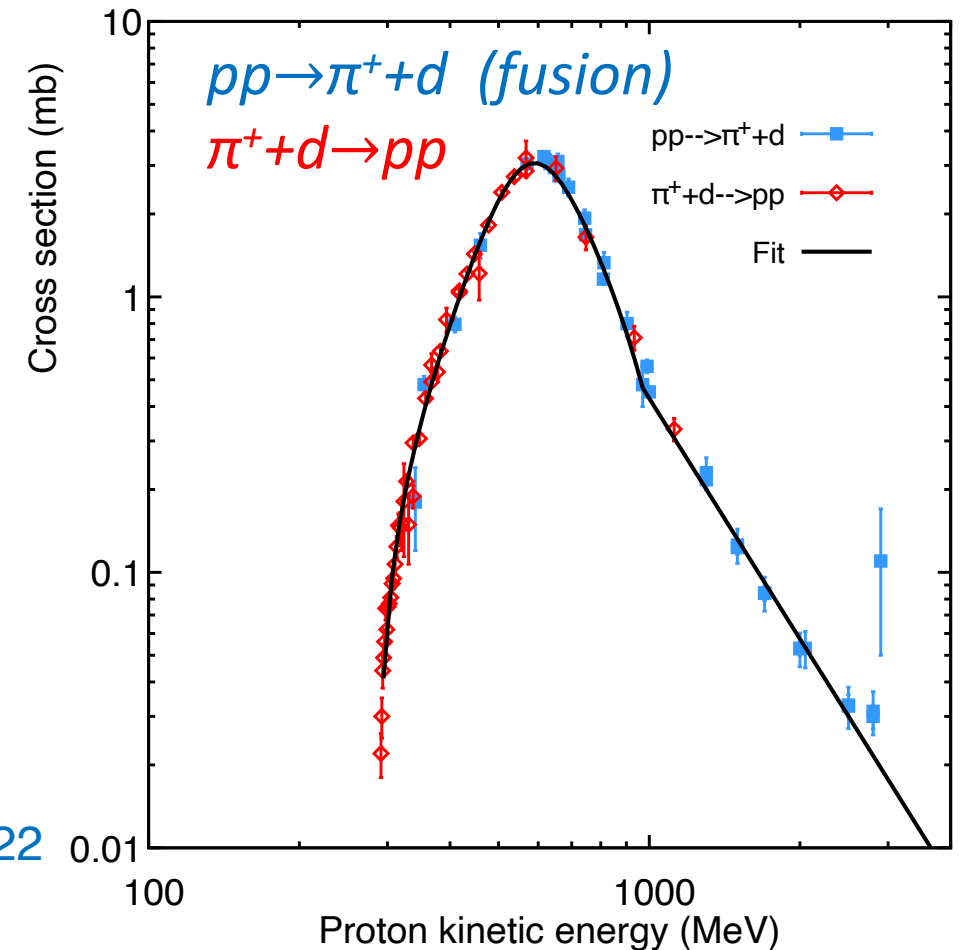
- Includes all $p+A$ and $\alpha+A$ reactions
- ${}^4\text{He}$ is the main progenitor



Porter+2022

Principle of detailed balance
(direct & inverse reactions):

$$\frac{\sigma_{pp}}{\sigma_{\pi d}} = 2 \frac{(2S_{\pi} + 1)(2S_d + 1)}{(2S_p + 1)^2} \frac{p'^2_{\pi}}{p'^2_p} = \frac{3}{2} \frac{p'^2_{\pi}}{p'^2_p}$$



Updated isotopic production cross sections

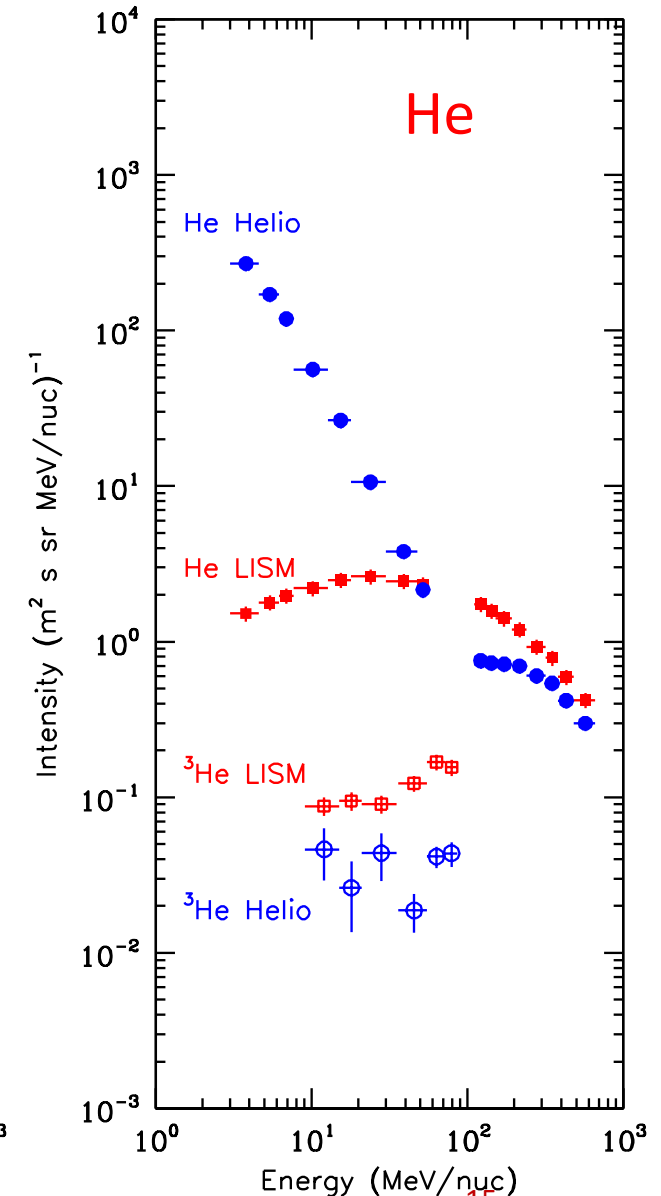
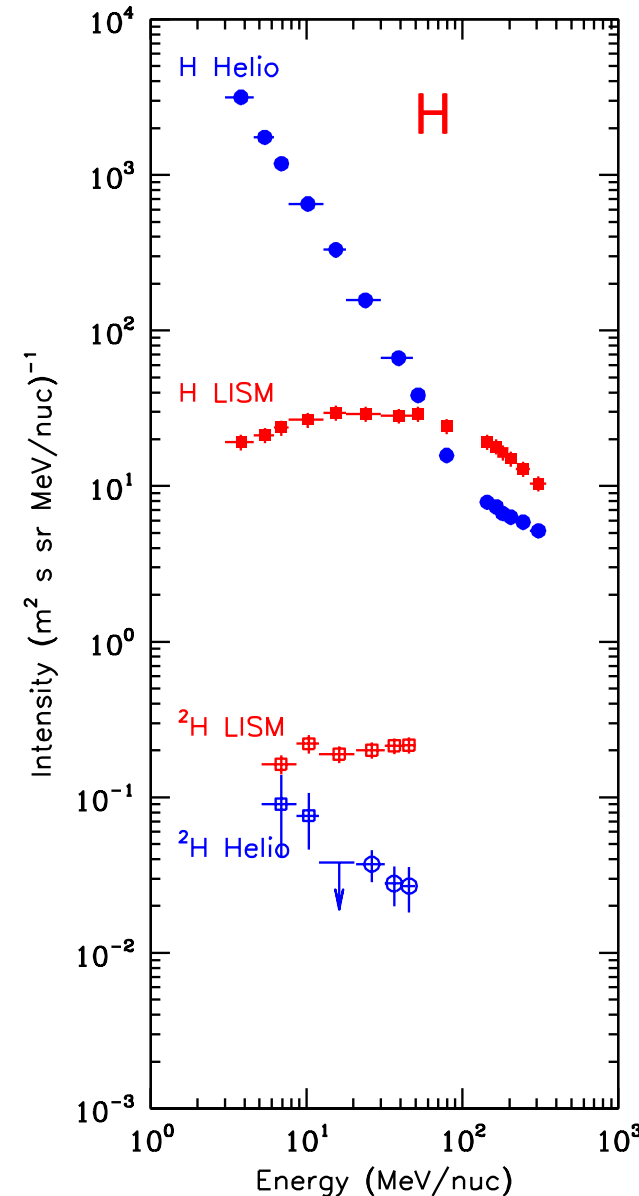
Table 3. Most significant reevaluated and updated production cross sections

Targets	$p + A \rightarrow B$	Reaction Products	Isotopes of Interest
${}^7\text{Li}$, ${}^7,9\text{Be}$, ${}^{10,11}\text{B}$, ${}^{12,13}\text{C}$, ${}^{14,15}\text{N}$, ${}^{16}\text{O}$, ${}^{56}\text{Fe}$	\rightarrow	${}^6,7\text{Li}$, ${}^7\text{Be}$	${}^6,7\text{Li}$
${}^9\text{Be}$, ${}^{10,11}\text{B}$, nat, ${}^{12,13}\text{C}$, nat, ${}^{14,15}\text{N}$, nat, ${}^{16}\text{O}$, nat, ${}^{24}\text{Mg}$, nat, ${}^{28}\text{Si}$, nat, ${}^{32}\text{S}$, nat, ${}^{56}\text{Fe}$	\rightarrow	${}^{7,9,10}\text{Be}$, ${}^{10}\text{B}$, ${}^{10}\text{C}$	${}^{7,9,10}\text{Be}$
${}^{11}\text{B}$, nat, ${}^{12,13}\text{C}$, nat, ${}^{14,15}\text{N}$, nat, ${}^{16}\text{O}$, ${}^{20,22}\text{Ne}$, nat, ${}^{24}\text{Mg}$, nat, ${}^{28}\text{Si}$, nat, ${}^{56}\text{Fe}$	\rightarrow	${}^{10}\text{Be}$, ${}^{10,11}\text{B}$, ${}^{10}\text{C}$	${}^{10,11}\text{B}$
nat, ${}^{14,15}\text{N}$, nat, ${}^{16}\text{O}$, ${}^{20,22}\text{Ne}$, nat, ${}^{24}\text{Mg}$, nat, ${}^{28}\text{Si}$, nat, ${}^{56}\text{Fe}$	\rightarrow	${}^{13}\text{C}$, ${}^{13}\text{N}$	${}^{13}\text{C}$
nat, ${}^{16}\text{O}$, ${}^{20,22}\text{Ne}$, nat, ${}^{24}\text{Mg}$, nat, ${}^{28}\text{Si}$, nat, ${}^{32}\text{S}$, nat, ${}^{56}\text{Fe}$	\rightarrow	${}^{15}\text{N}$, ${}^{15}\text{O}$	${}^{15}\text{N}$
${}^{19}\text{F}$, ${}^{20,22}\text{Ne}$, ${}^{23}\text{Na}$, nat, ${}^{24}\text{Mg}$, ${}^{27}\text{Al}$, nat, ${}^{28}\text{Si}$, nat, ${}^{32}\text{S}$, nat, ${}^{56}\text{Fe}$	\rightarrow	${}^{17}\text{C}$, ${}^{17}\text{N}$, ${}^{17,18}\text{O}$, ${}^{17,18}\text{F}$, ${}^{17,18}\text{Ne}$	${}^{17,18}\text{O}$
${}^{20,22}\text{Ne}$, ${}^{23}\text{Na}$, nat, ${}^{24}\text{Mg}$, nat, ${}^{28}\text{Si}$, nat, ${}^{32}\text{S}$, nat, ${}^{56}\text{Fe}$	\rightarrow	${}^{19}\text{F}$, ${}^{19}\text{Ne}$	${}^{19}\text{F}$
nat, ${}^{24}\text{Mg}$, ${}^{27}\text{Al}$, nat, ${}^{28}\text{Si}$, nat, ${}^{56}\text{Fe}$	\rightarrow	${}^{21,22}\text{Ne}$, ${}^{21,22}\text{Na}$	${}^{21,22}\text{Ne}$
nat, ${}^{48,49}\text{Ti}$, nat, ${}^{52}\text{Cr}$, nat, ${}^{56}\text{Fe}$	\rightarrow	${}^{45}\text{Ca}$, ${}^{45}\text{Sc}$, ${}^{45}\text{Ti}$	${}^{45}\text{Sc}$
nat, ${}^{52}\text{Cr}$, ${}^{55}\text{Mn}$, nat, ${}^{56}\text{Fe}$	\rightarrow	${}^{47}\text{Ca}$, ${}^{46,47,48,49,50}\text{Sc}$, ${}^{44,46,47,48,49,50,51}\text{Ti}$, ${}^{46,47,48,49,50,51}\text{V}$, ${}^{48,49,51}\text{Cr}$, ${}^{49,51,54}\text{Mn}$	${}^{44,46,47,48,49,50}\text{Ti}$, ${}^{50,51}\text{V}$

Will be available with the next version of GALPROP

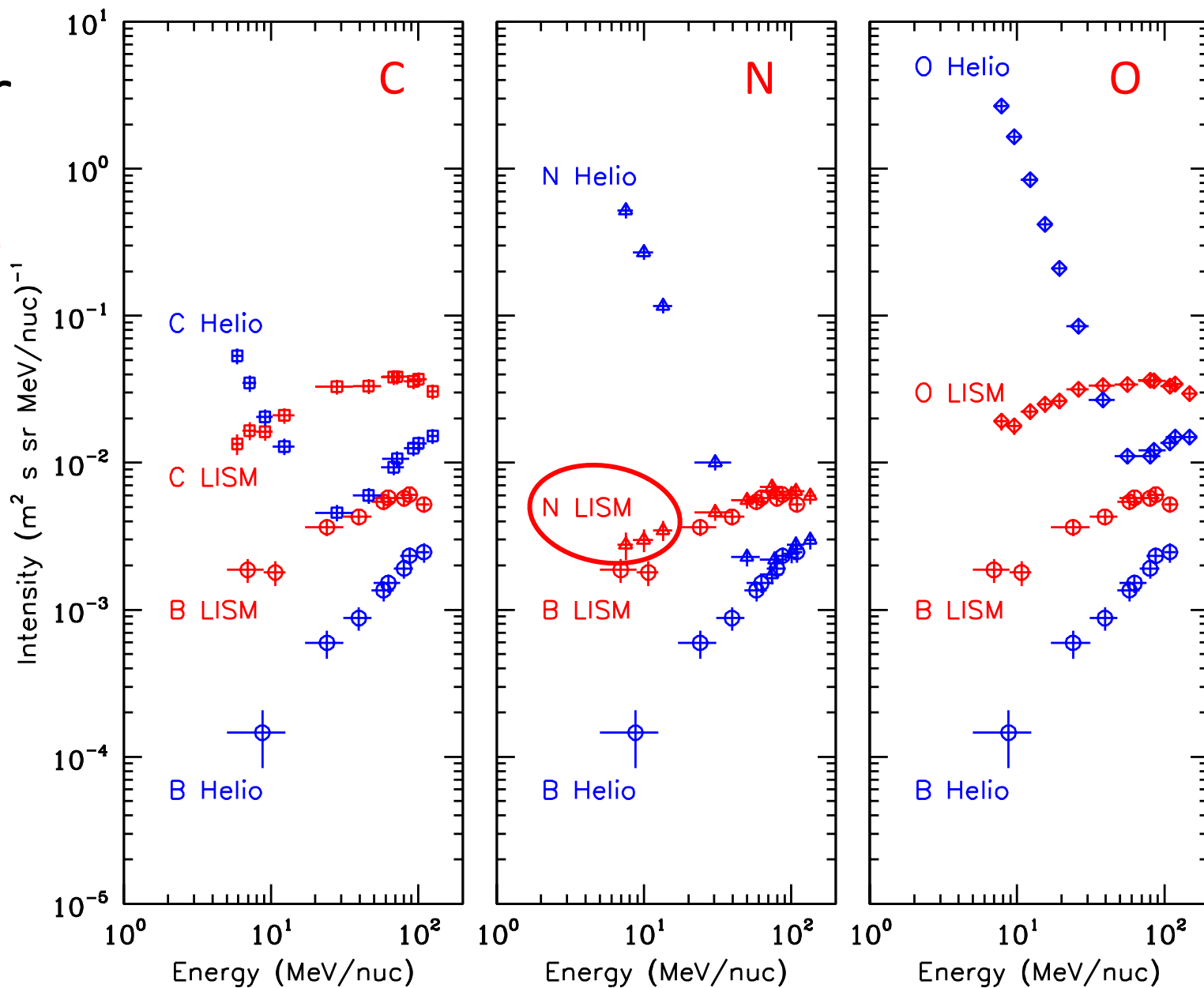
Why ^2H excess is not instrumental

- Energy spectra in the heliosheath (blue) and in the very local ISM (red)
- Below 50 MeV/nuc the anomalous CR (ACR) He intensity in the heliosheath is much larger than the GCR intensity in the very local ISM
- ^4He is the main progenitor of ^2H (and ^3He) in CRs. Assume same for mylar/sheldahl windows
- Yet, with higher ACR He intensity below 50 MeV/nuc, the ^2H intensity in the heliosheath is lower, not higher, than in the very local ISM !
- This is the strongest argument as to why nuclear interactions in the windows are not responsible for the excess ^2H



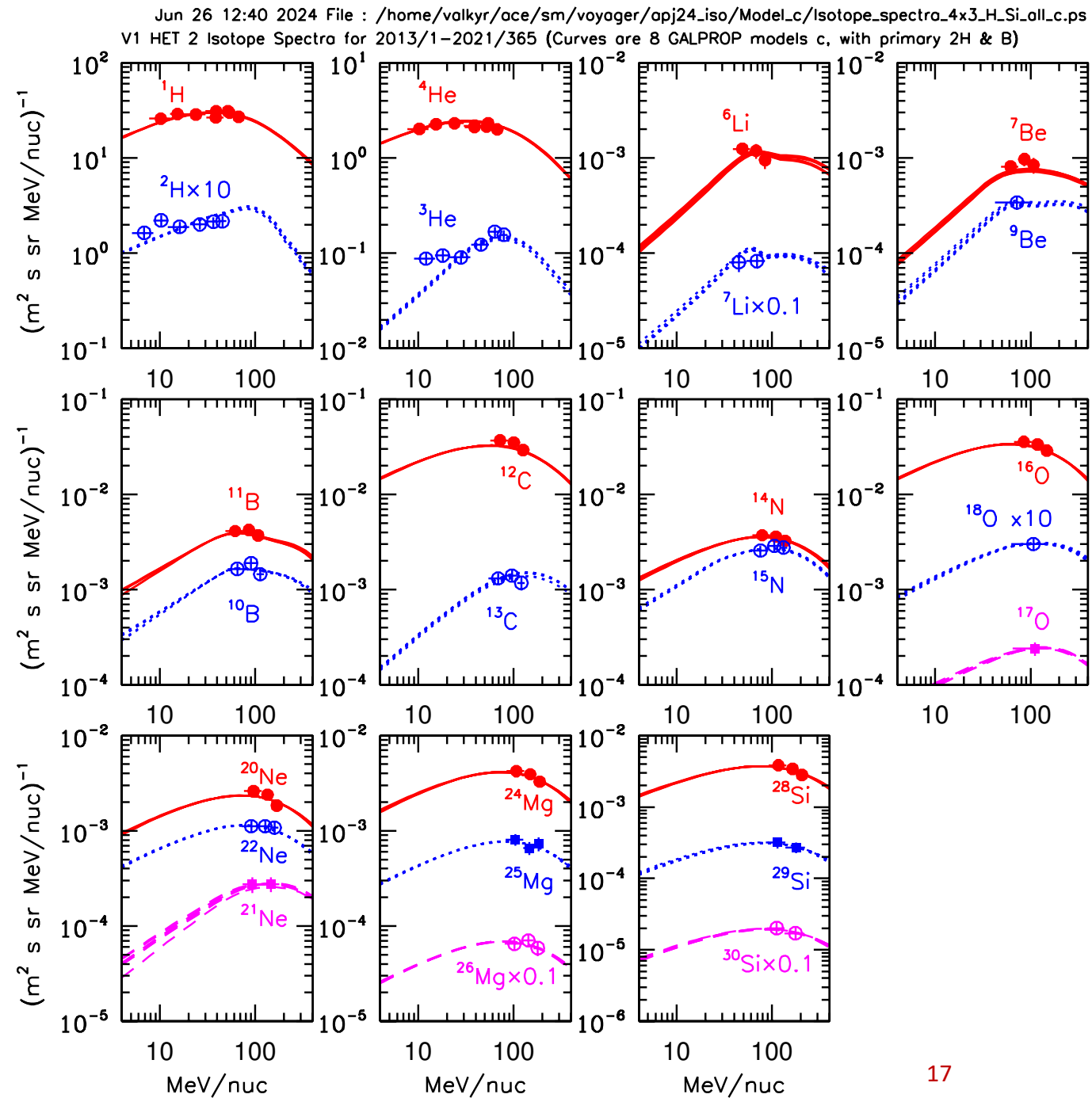
Boron is not instrumental either

- Energy spectra in the heliosheath (blue) and in the very local ISM (red)
- Below 50 MeV/nuc the anomalous CR (ACR) CNO intensity in the heliosheath is much larger than the GCR intensity in the very local ISM
- CNO are the main progenitors of B
- Yet, with higher ACR CNO intensity below 50 MeV/nuc, the B intensity in the heliosheath is lower, not higher, than in the very local ISM!
- This is the strongest argument as to why nuclear interactions in the windows are not responsible for the excess B



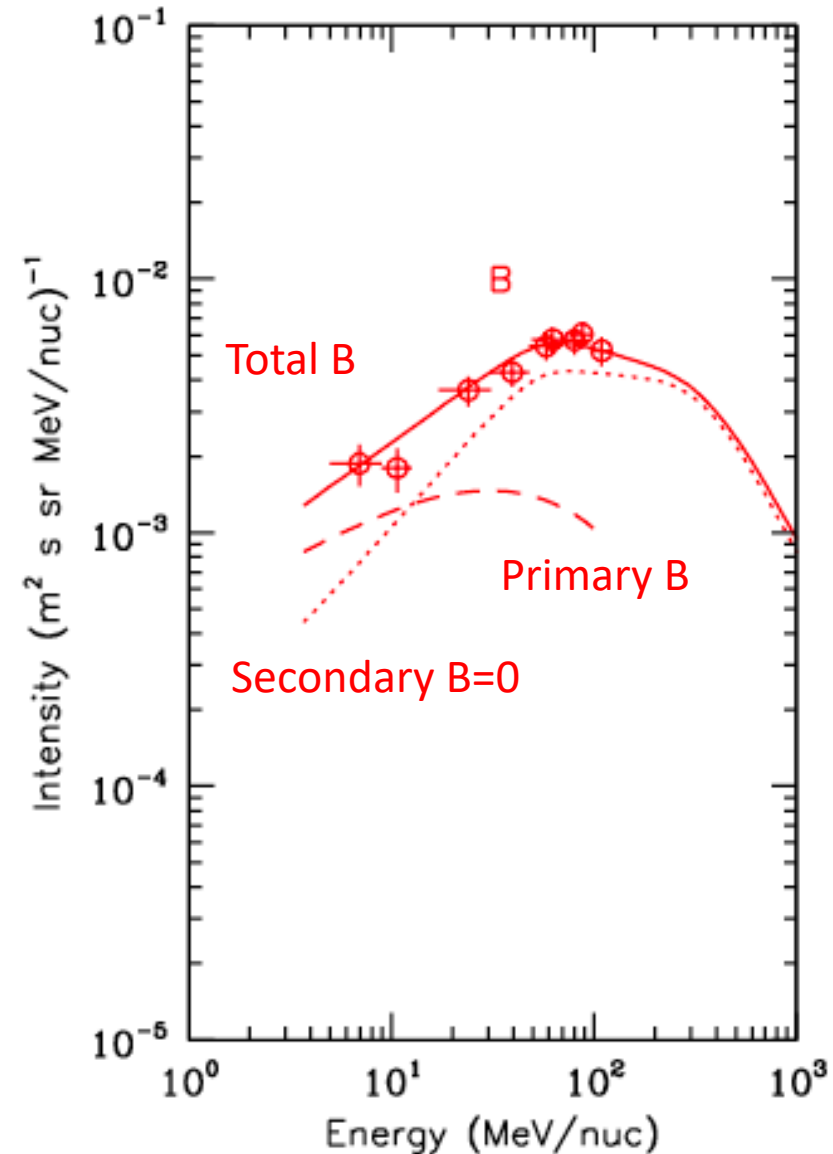
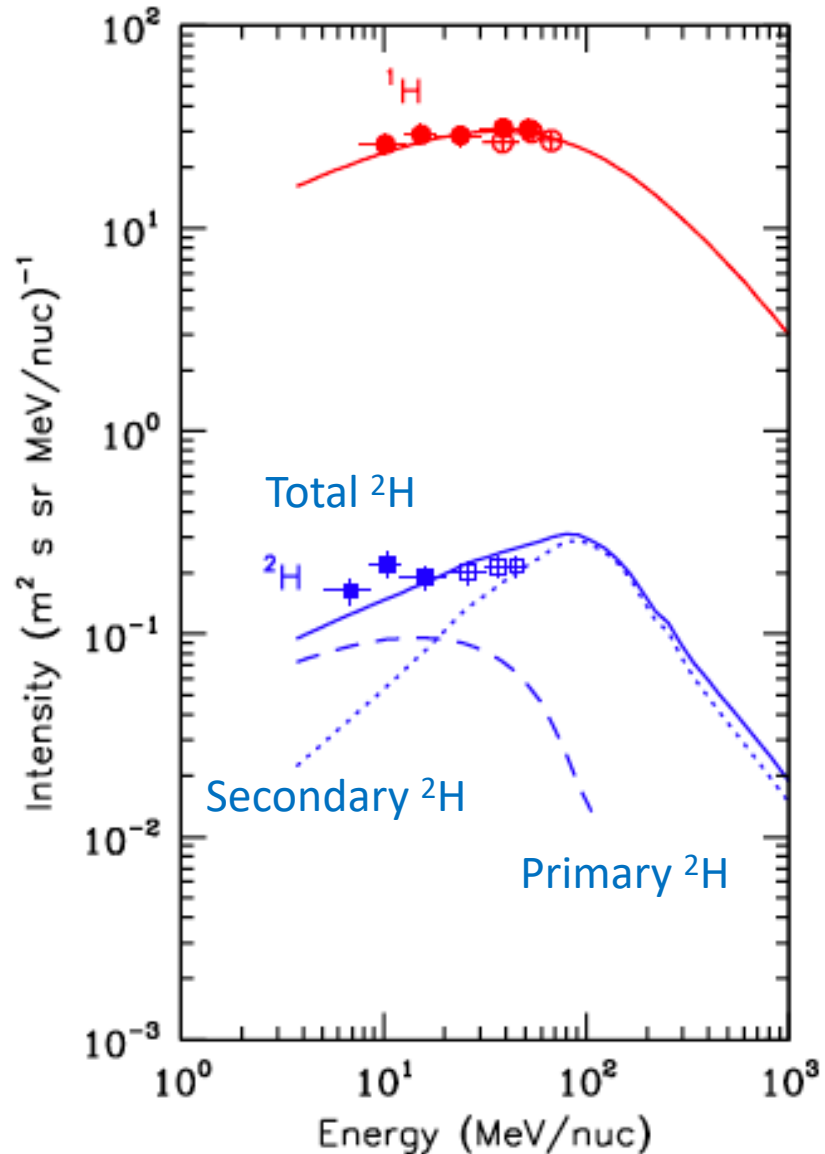
Primary ^2H and B

- Allow free abundances of ^2H and B (^3He , Li, Be = 0)
- Again 8 GALPROP models
- Good fit for all species for all 8 models including ^2H and B
- Origin of primary ^2H (Caselli & Ceccarelli 2012)
 - Deuteration of organic molecules and dust grain surfaces
 - Deuterium released under heating or passing shock (Linsky+2006)



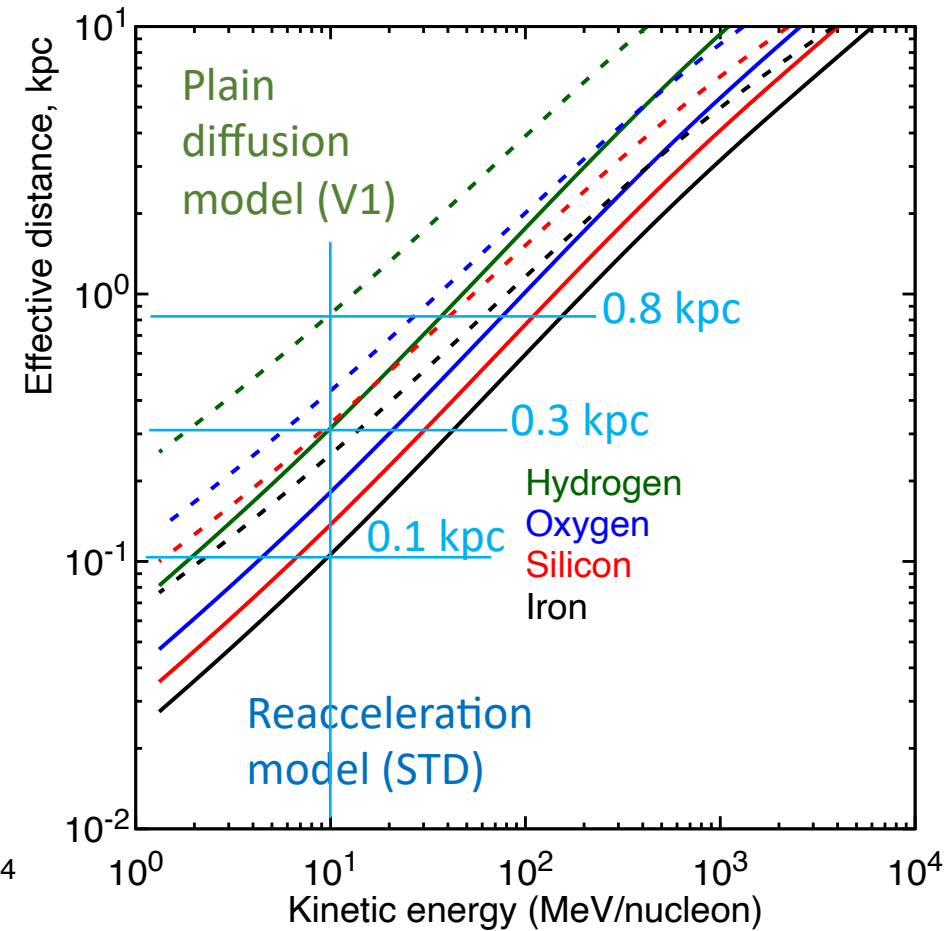
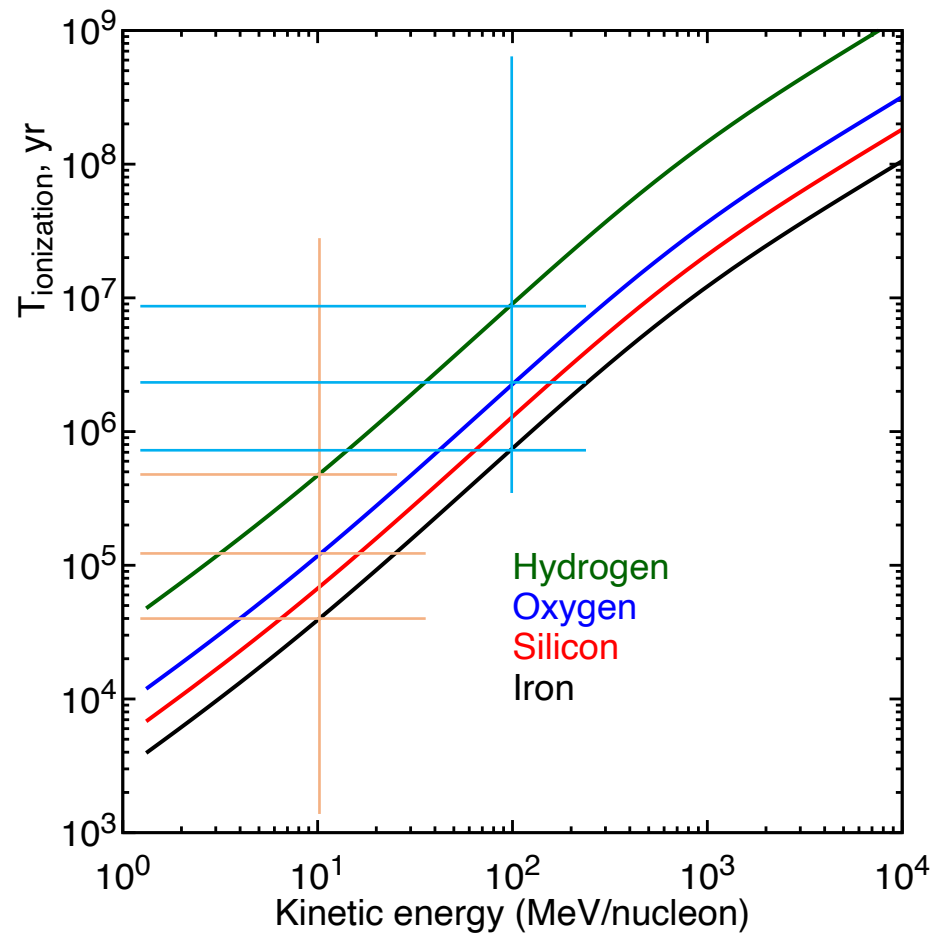
- $^2\text{H}/^1\text{H}$ abundance ratio can vary by orders of magnitude in different environments
- In the gas phase $^2\text{H}/^1\text{H}$ ratio is $\sim 10^{-5}$ – close to the primordial ratio
- Organic molecules and dust grain surfaces show enhancements of the $^2\text{H}/^1\text{H}$ ratio of up to **13 orders of magnitude** with respect to the elemental $^2\text{H}/^1\text{H}$ abundance ratio (i.e. in the form of H, D, H_2 , D_2 , HD)
- $^2\text{H}/^1\text{H} \sim 0.1\text{--}1$ values are quite common
- The origin of such enhancements and the complex deuterium chemistry on the dust grain surfaces is widely discussed in the literature ([Caselli & Ceccarelli 2012](#))

Primary ^2H & B



Ionization energy losses and propagation distance

- Coulomb losses not included
- $n_H \sim 1 \text{ cm}^3$, $\text{He}/\text{H}=0.1$
- The timescale $< 100 \text{ yr}$ (10 MeV/n, Fe) to $\sim 10 \text{ Myr}$ (100 MeV/n, H)
- The effective propagation distances (**upper limit**) at 10 MeV/n: from 0.8 kpc (H) to 0.1 kpc (Fe) in different models
- At 100 MeV/n it is $< 2 \text{ kpc}$ for most species



AMS-02 reports of the primary component in ^2H

PHYSICAL REVIEW LETTERS **132**, 261001 (2024)

Editors' Suggestion

Featured in Physics

Properties of Cosmic Deuterons Measured by the Alpha Magnetic Spectrometer

M. Aguilar,²⁹ B. Alpat,³⁵ G. Ambrosi,³⁵ H. Anderson,¹⁰ L. Arruda,²⁷ N. Attig,²⁴ C. Bagwell,¹⁰ F. Barao,²⁷ M. Barbanera,³⁵

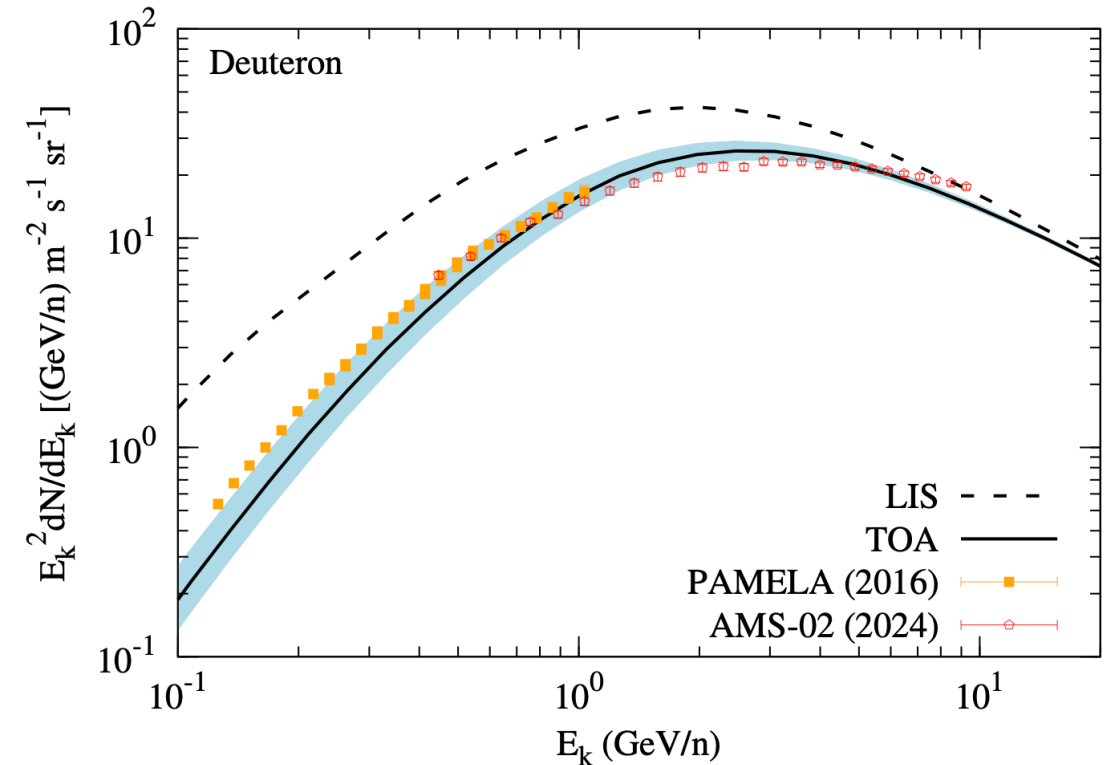
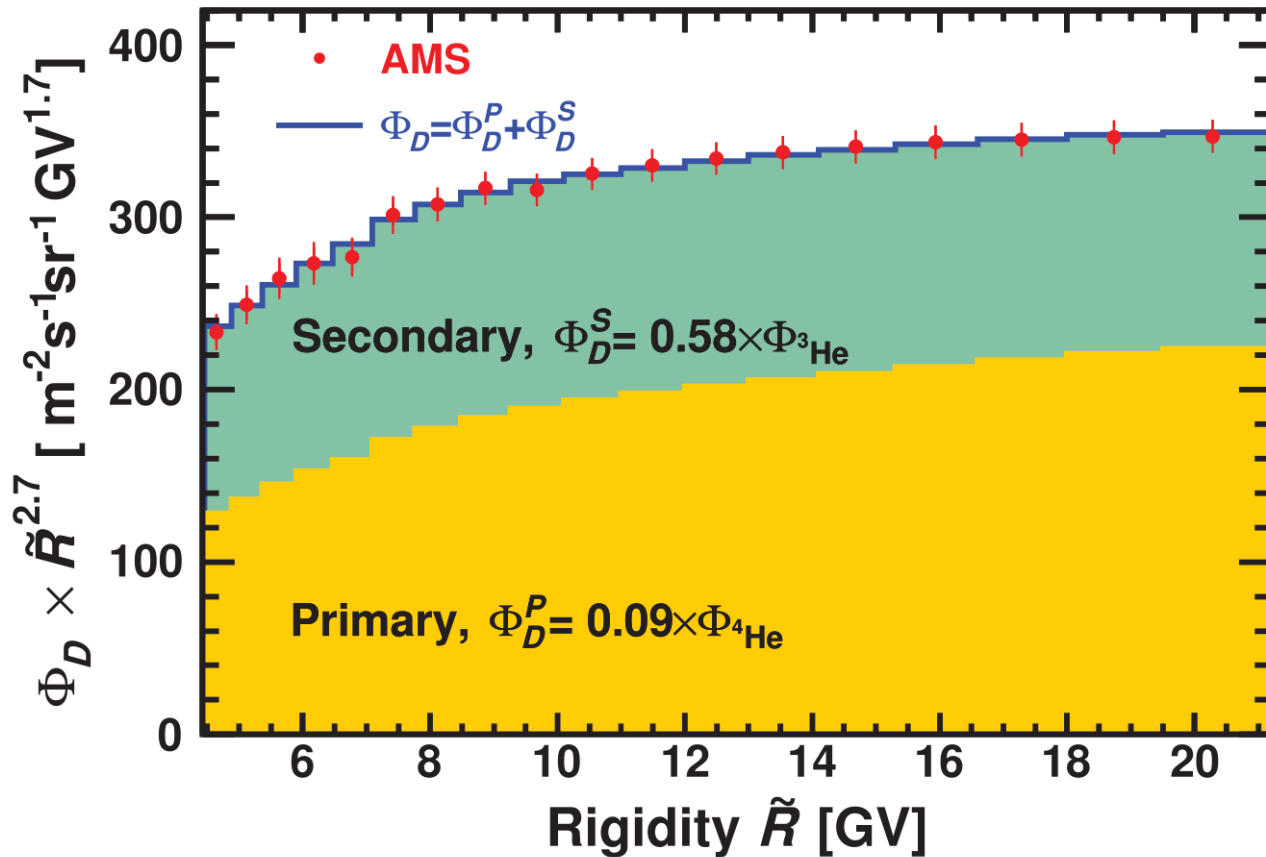
Above ~ 13 GV we find a nearly identical rigidity dependence of the D and p fluxes with a D/p flux ratio of 0.027 ± 0.001 . These unexpected observations indicate that cosmic deuterons have a sizable primarylike component. With a method independent of cosmic ray propagation, we obtain the primary component of the D flux equal to $9.4 \pm 0.5\%$ of the ^4He flux and the secondary component of the D flux equal to $58 \pm 5\%$ of the ^3He flux.

The AMS-02 cosmic ray deuteron flux is consistent with a secondary origin

Qiang Yuan^{1,2,*} and Yi-Zhong Fan^{1,2,†}

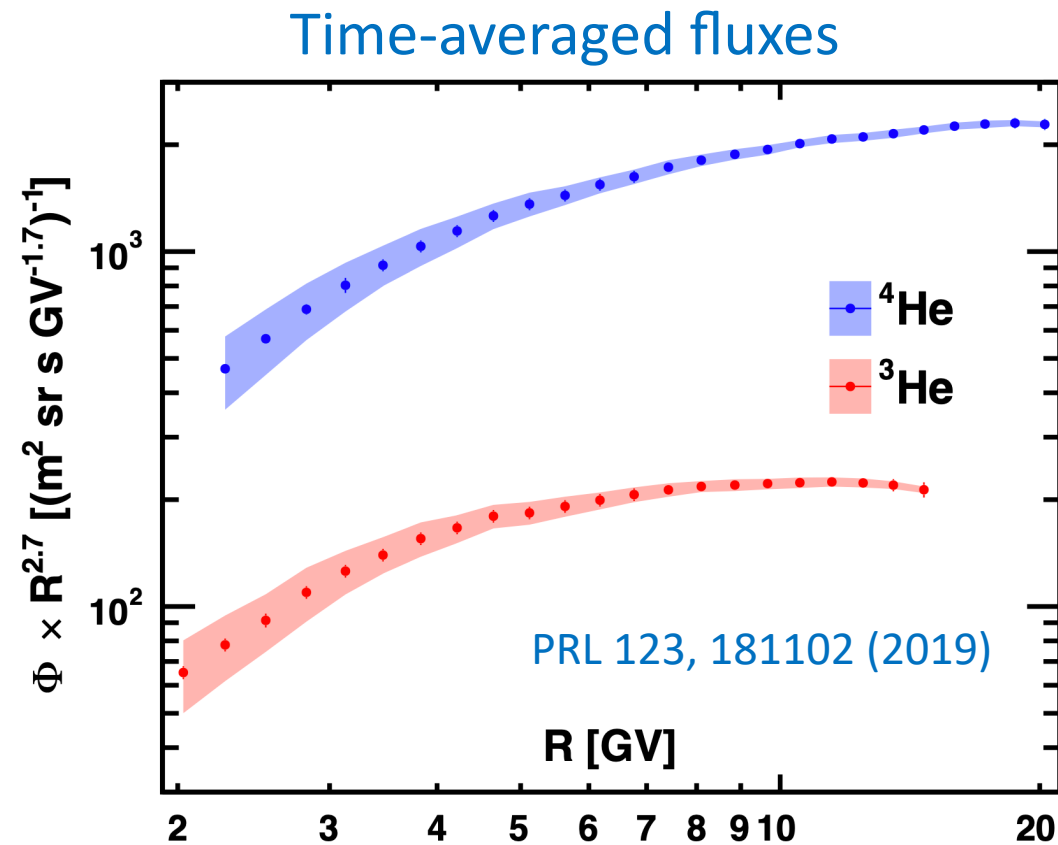
arXiv: 2406.19315

AMS-02, PRL 2024



GALPROP v56 with D cross sections updated
Contributions of H-Fe are important

AMS-02: Helium-3 excess



Helium-3

Standard parameters:

- Same propagation parameters used for all species $^1\text{H} - ^{64}\text{Ni}$
- Tuned using the B/C and $^{10}\text{Be}/^9\text{Be}$ ratios

Alternative propagation:

- Derived from the fit to the $^3\text{He}/^4\text{He}$ ratio
- Halo size fixed at 4 kpc
- Secondary ^3He production by $Z>2$ species is calculated with the standard parameters

Table 1. Best-fit propagation parameters for *I*- and *P*-scenarios

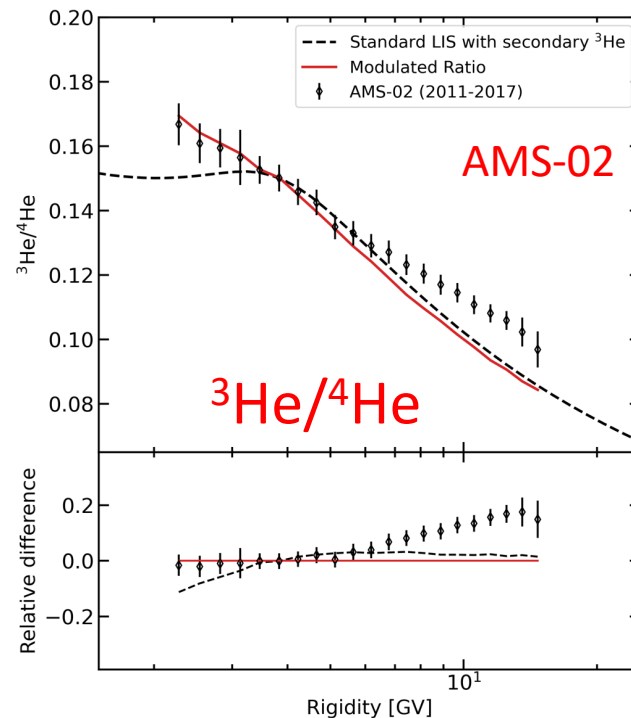
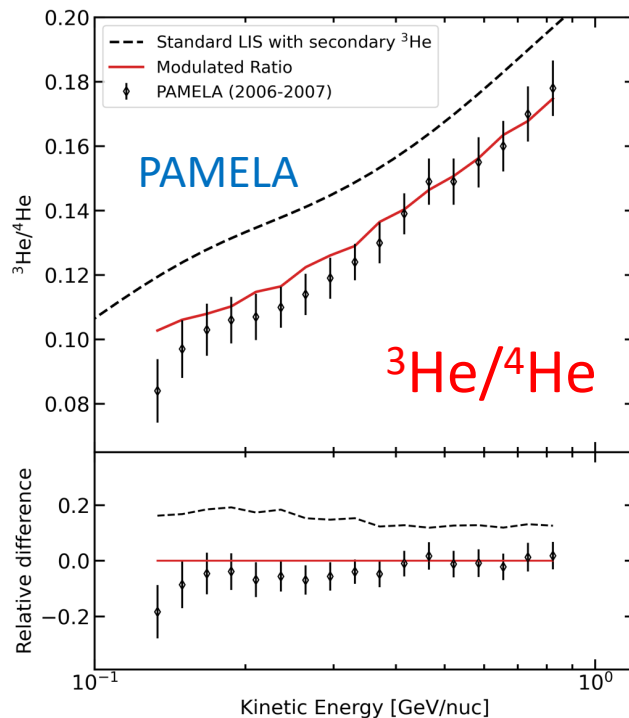
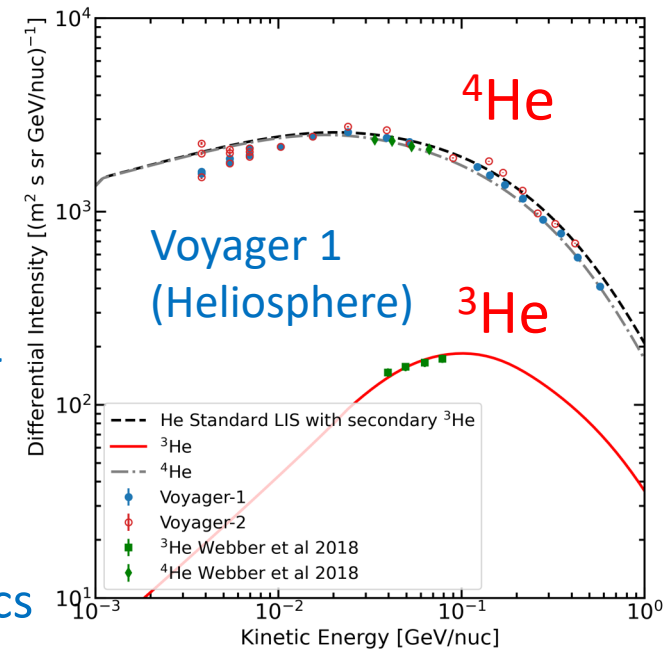
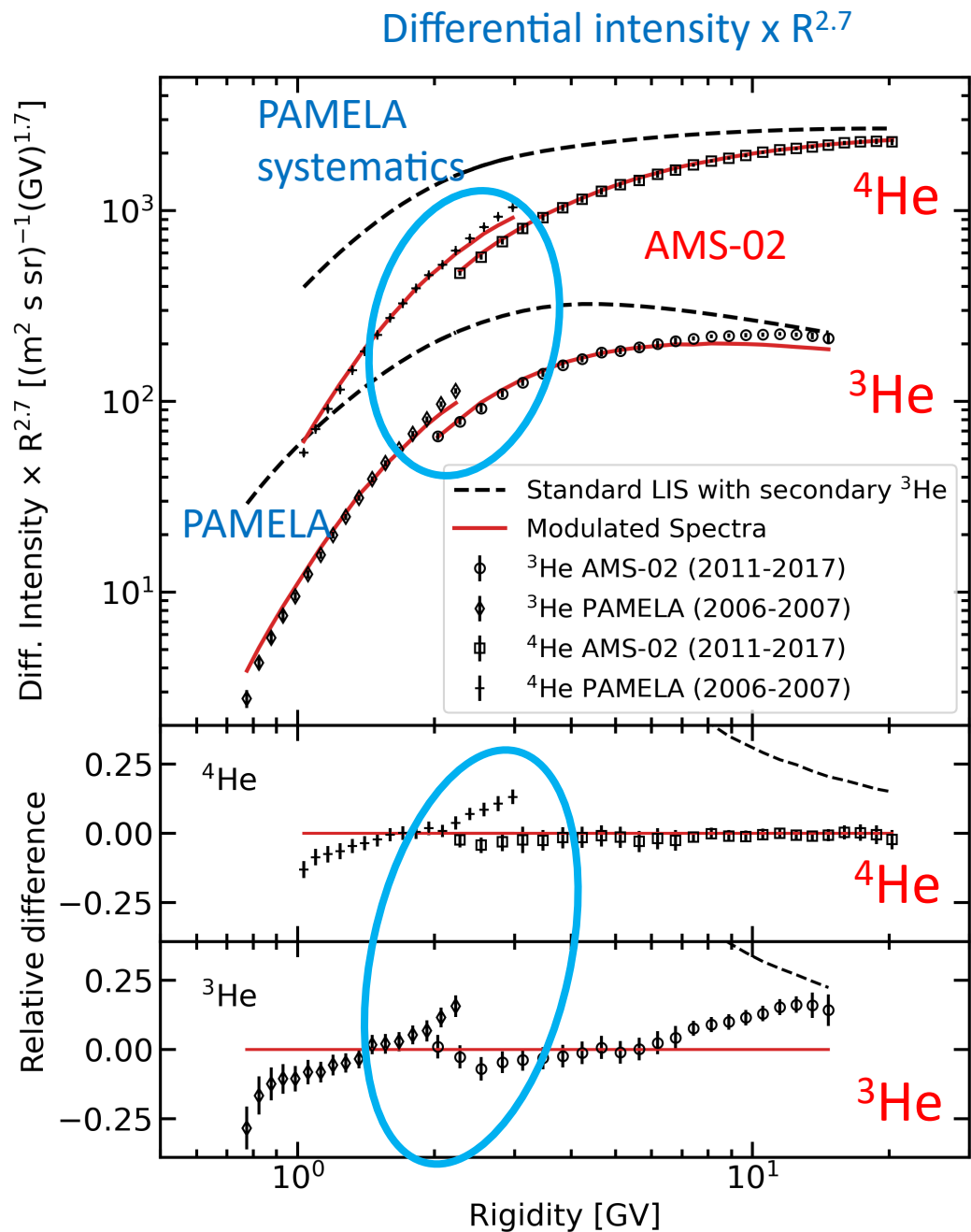
Parameter	Units	Model	
		Standard	Alternative
z_h	kpc	4.0 ± 0.6	4.0 (fixed)
$D_0(R = 4 \text{ GV})$	$10^{28} \text{ cm}^2 \text{ s}^{-1}$	4.3 ± 0.7	5.9 ± 1.0
δ	...	0.415 ± 0.025^a	0.19 ± 0.06
V_{Alf}	km s^{-1}	30 ± 3	27.3 ± 5
dV_{conv}/dz	$\text{km s}^{-1} \text{ kpc}^{-1}$	9.8 ± 0.8	2 ± 2
η	...	0.70	1.2

^aThe *P*-scenario assumes a break in the diffusion coefficient with index $\delta_1 = \delta$ below the break and index $\delta_2 = 0.15 \pm 0.03$ above the break at $R = 370 \pm 25 \text{ GV}$ (for details see [Boschini et al. 2020b](#)).

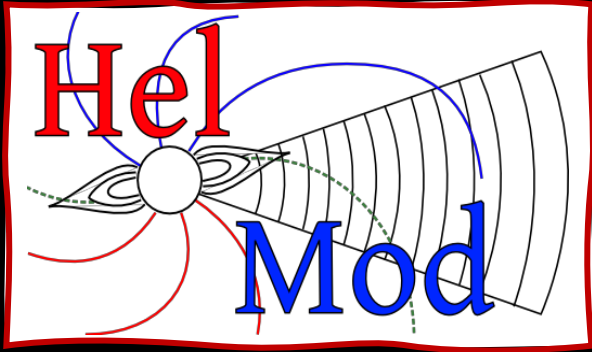
Standard model calcs

PAMELA Systematics:

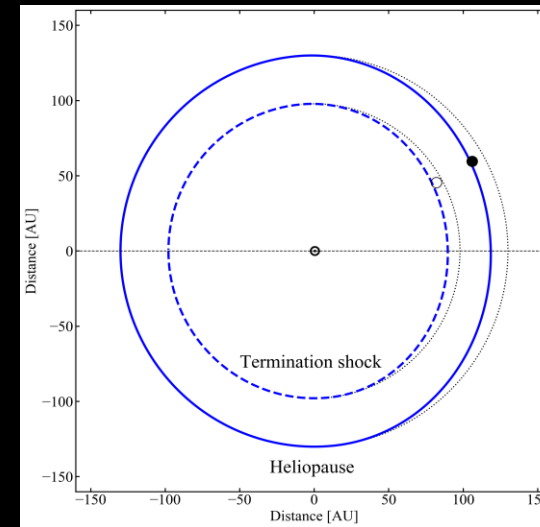
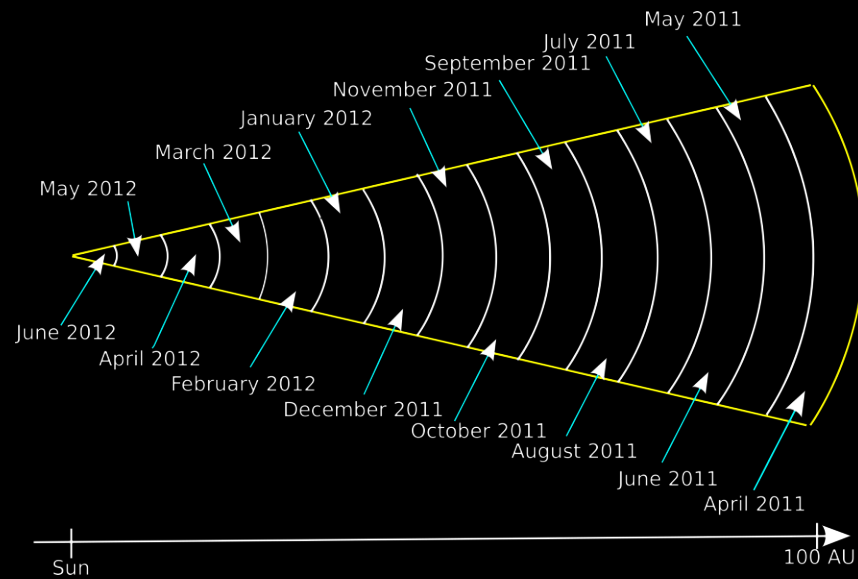
- Difference between PAMELA & AMS-2 should decrease with rigidity, but it increases
- The PAMELA $^3\text{He}/^4\text{He}$ ratio looks right – cancels systematics



The HelMod Perspective



The HelMod Model evaluates the solar modulation through the heliosphere. The Model is continuously updated, including, e.g., the shape of the outer heliosphere, and time variation of rigidity dependence of diffusion tensors...



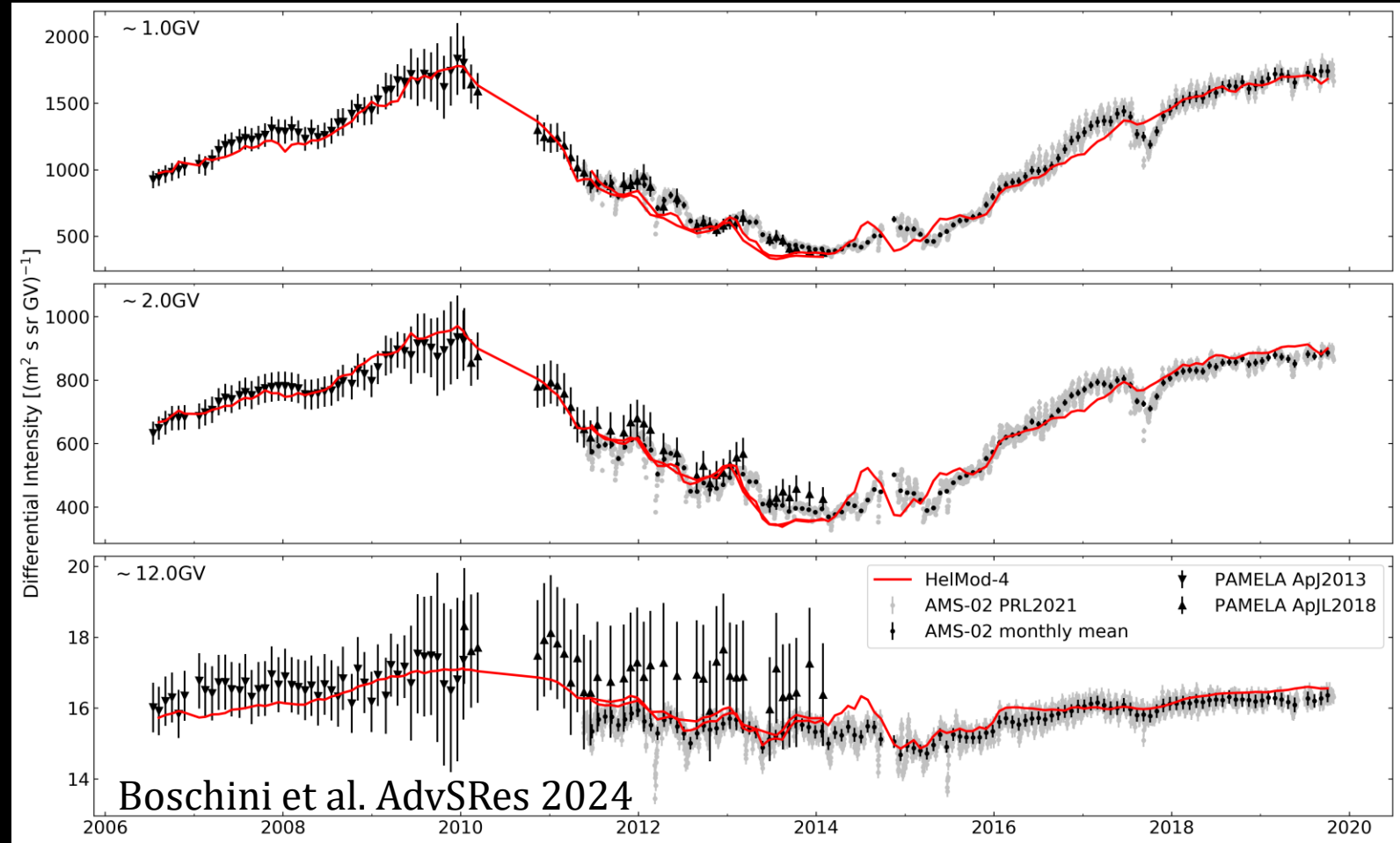
The model describes the interplanetary medium following the solar disturbances propagation time from the Sun.

The HelMod Perspective

Model parameters are tuned along a complete 22-year solar cycle using CR proton data with the highest statistics and lowest systematics.

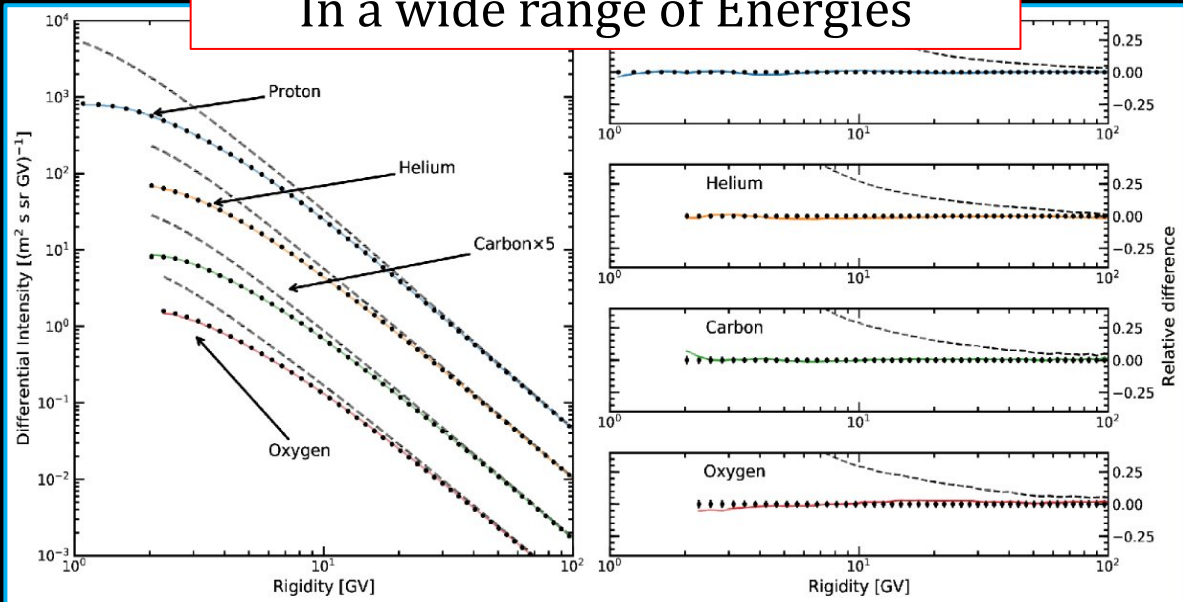
The same parametrization is then applied to all nuclei.

Latest updated, HelMod-4 (v5.1), was tuned including AMS-02 daily proton flux up to 2019

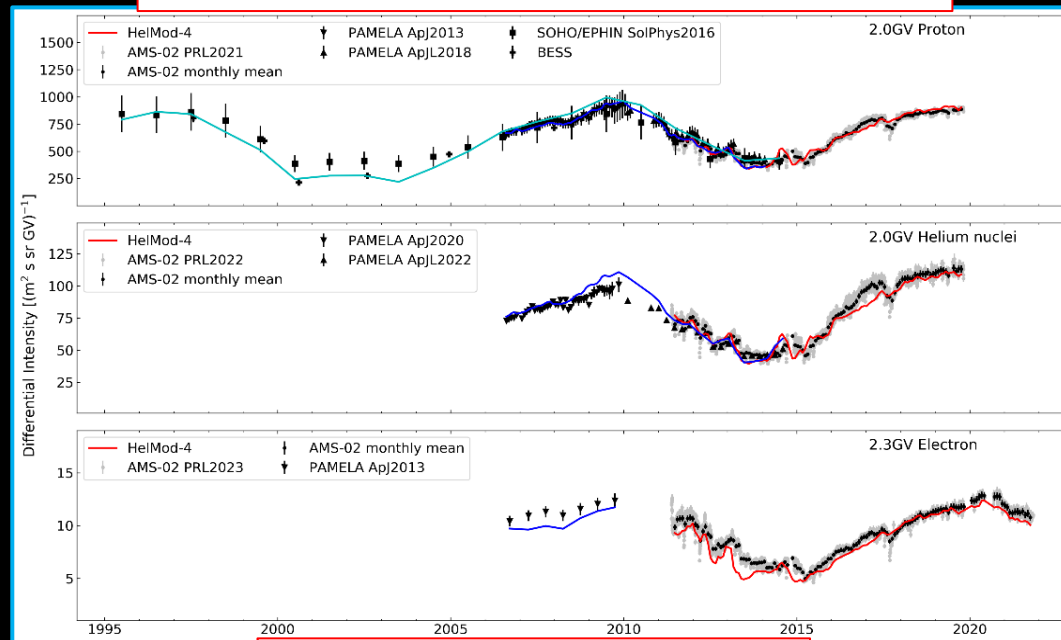


HelMod reproduces Ions:

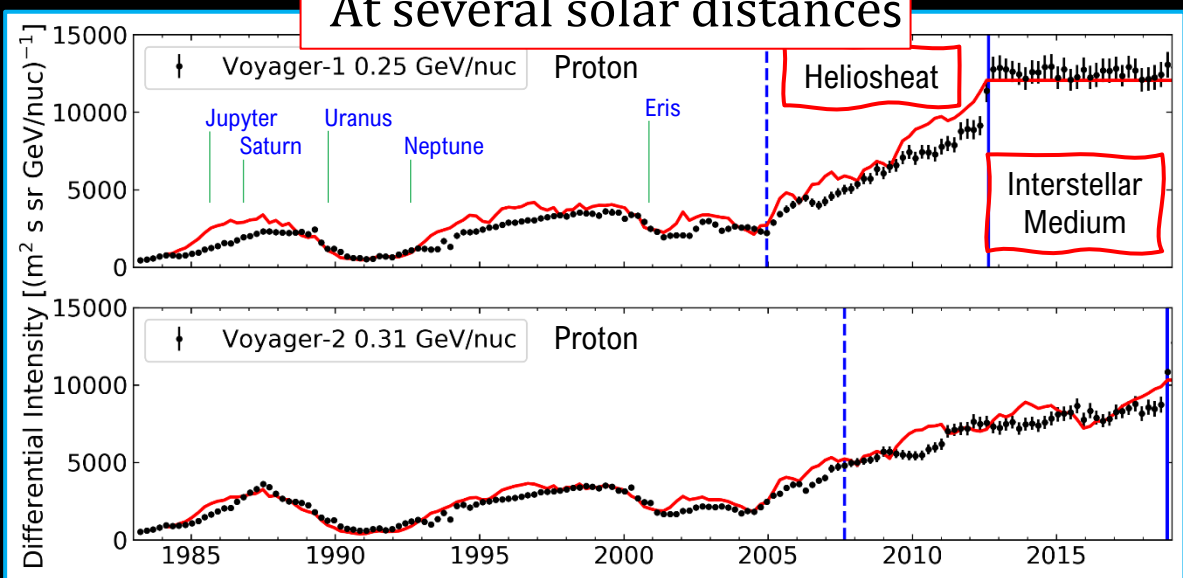
In a wide range of Energies



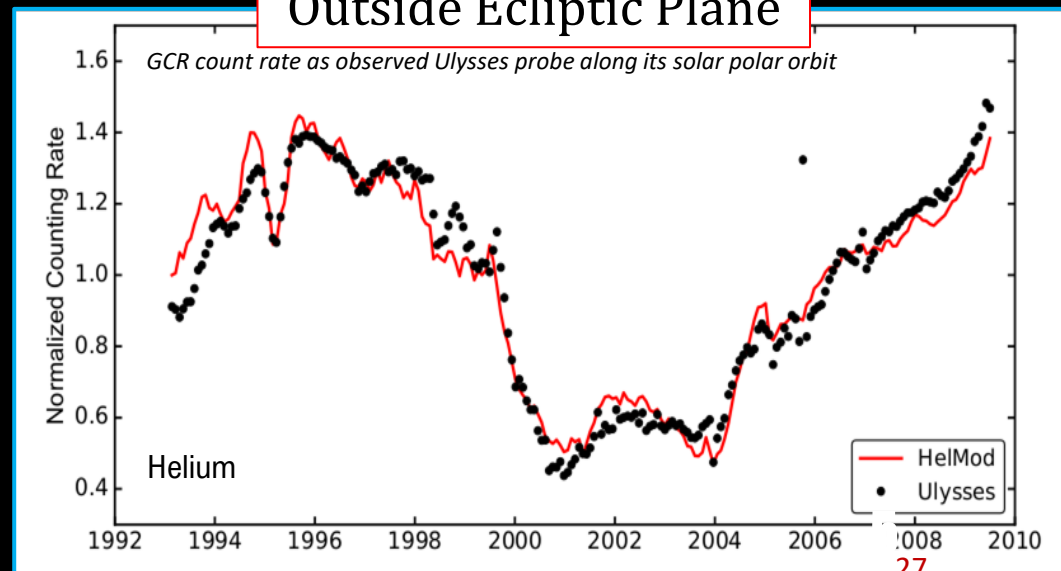
For different solar activities



At several solar distances

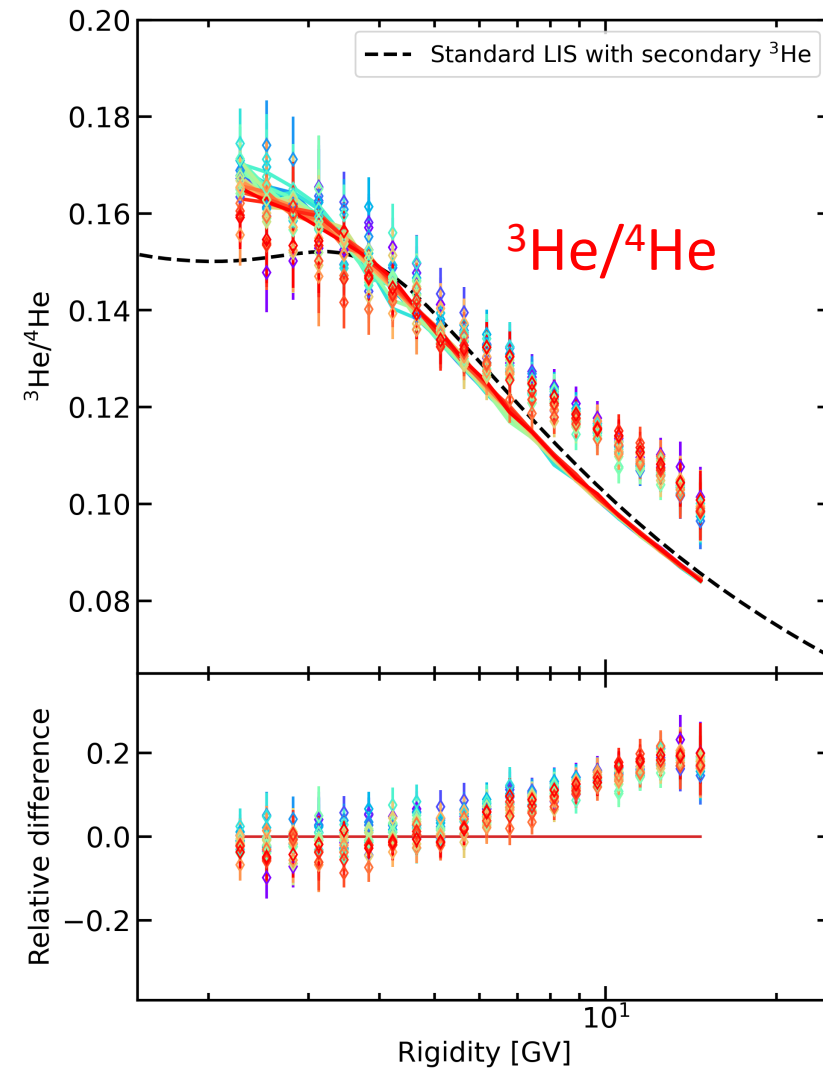
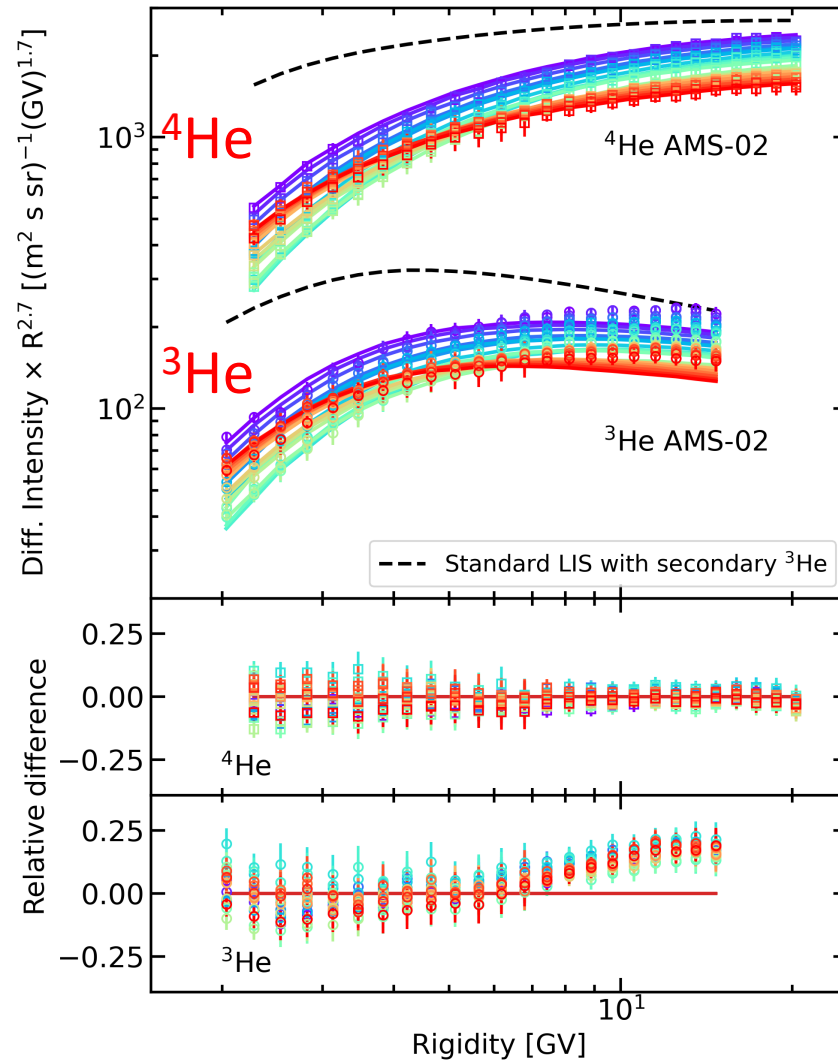


Outside Ecliptic Plane

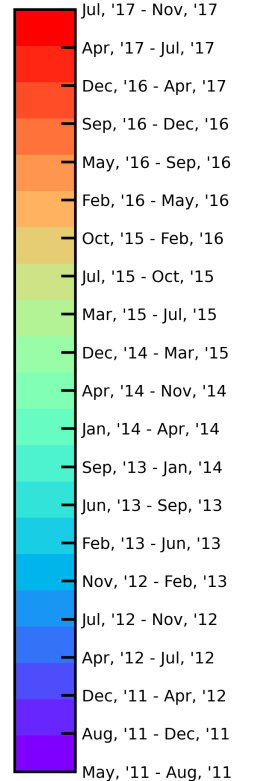


Variations over the solar cycle (AMS-02)

Calculations made in standard model for Bartel rotation overaged fluxes – all show the excess in ^3He



Bartel rotations

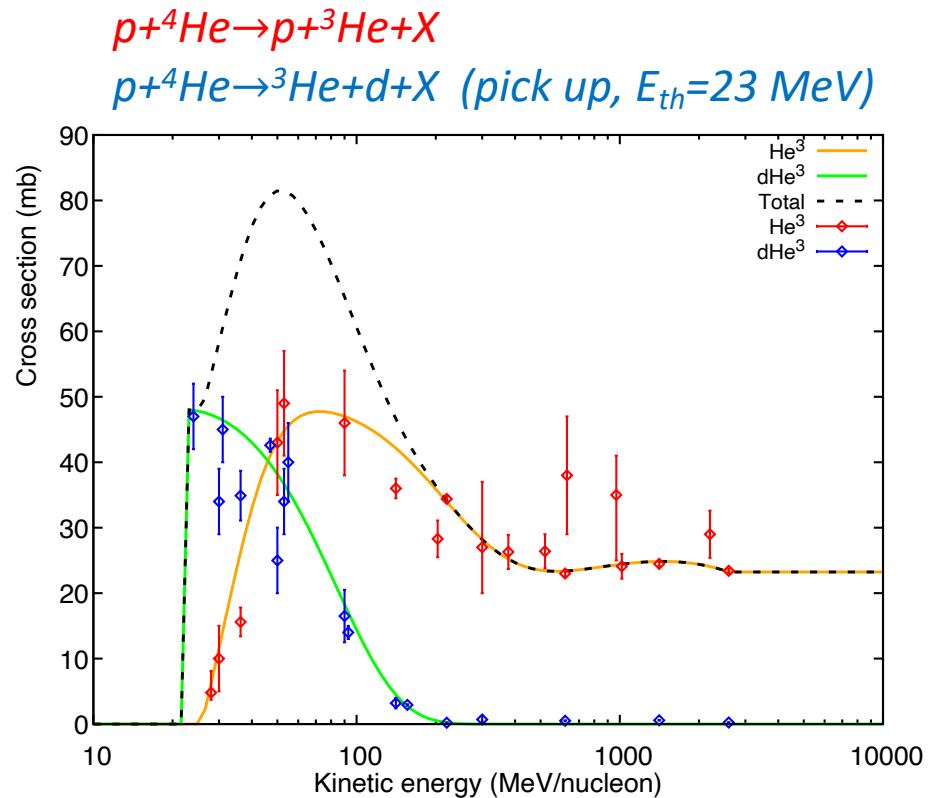


Hypotheses of the origin of ^3He excess

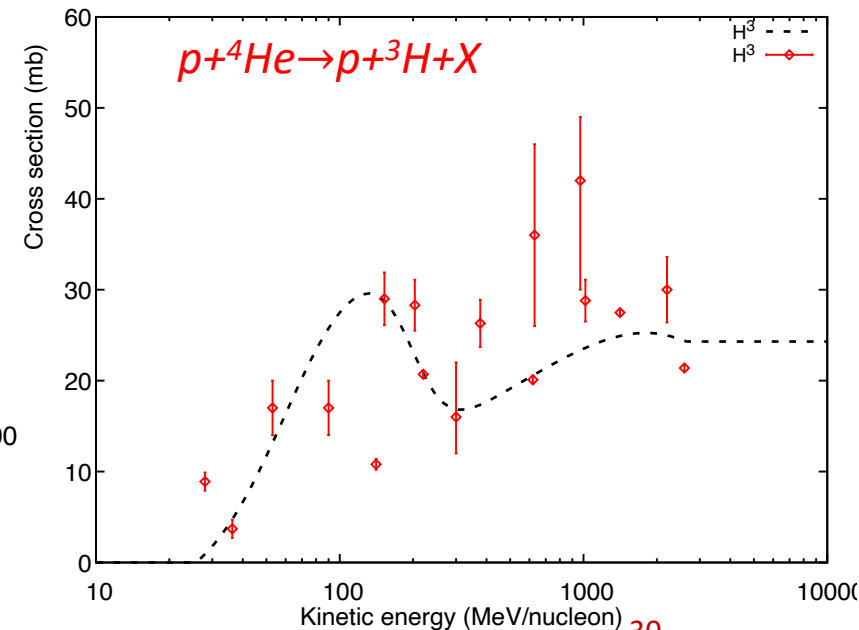
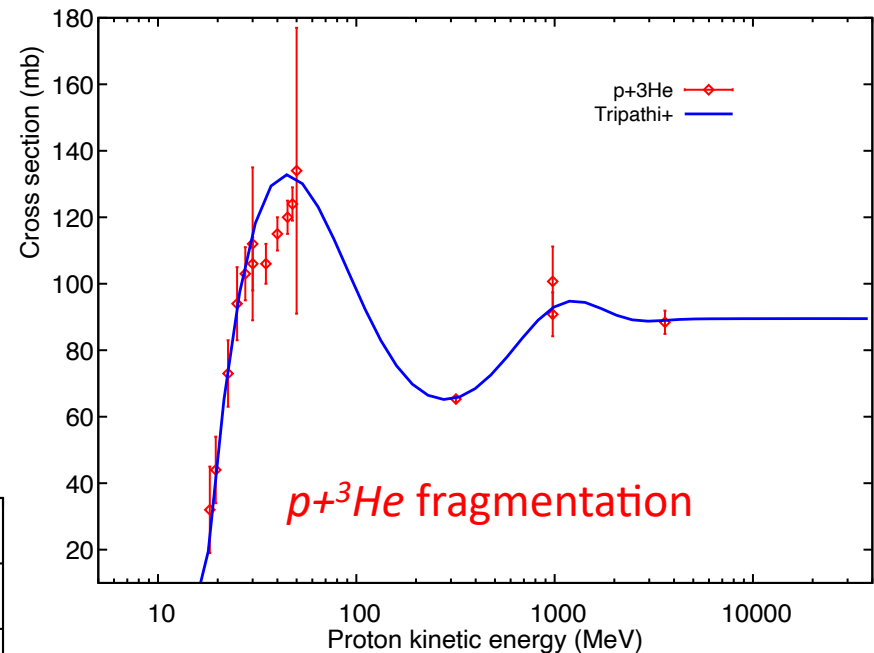
- i. Accuracy of ^3He production and fragmentation Xsections
- ii. Primary ^3He component with a harder injection spectrum
- iii. A non-uniform propagation probed on different spatial scales by light isotopes ($^3,^4\text{He}$) and heavier species (e.g., the B/C ratio)

- v57 includes all $p+A$ and $\alpha+A$ reactions
- ^4He is the main progenitor
- All Xsections are flat above ~ 2 GeV/n
- Agree below 7 GV
- Excess – above 7 GV (^3He : >3.8 GeV/n, ^4He : >2.7 GeV/n)
- Thus, the **energy-independent (rigidity-independent) Xsections** cannot be the reason of the **observed rigidity-dependent ^3He excess**

I. ^3He cross sections (GALPROP v57)



Porter+2022

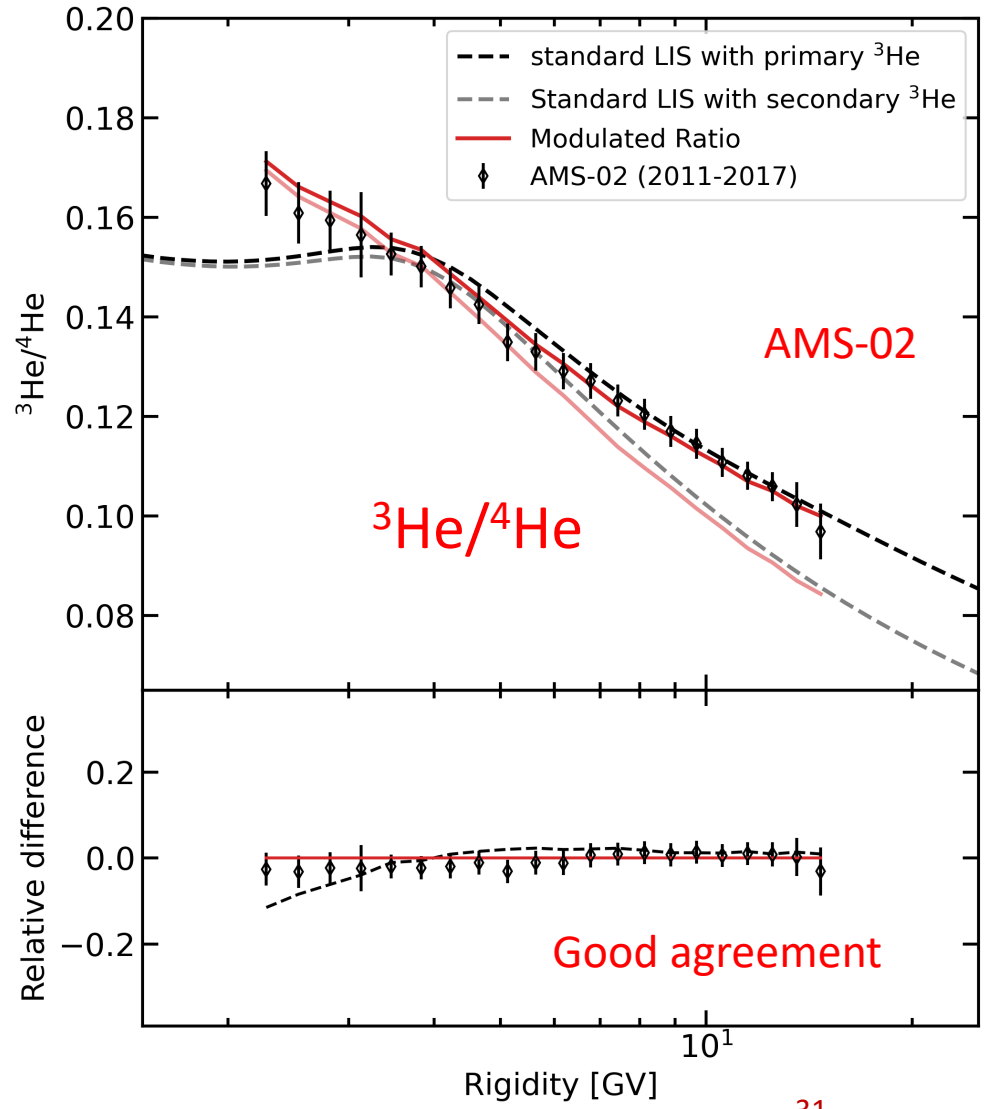
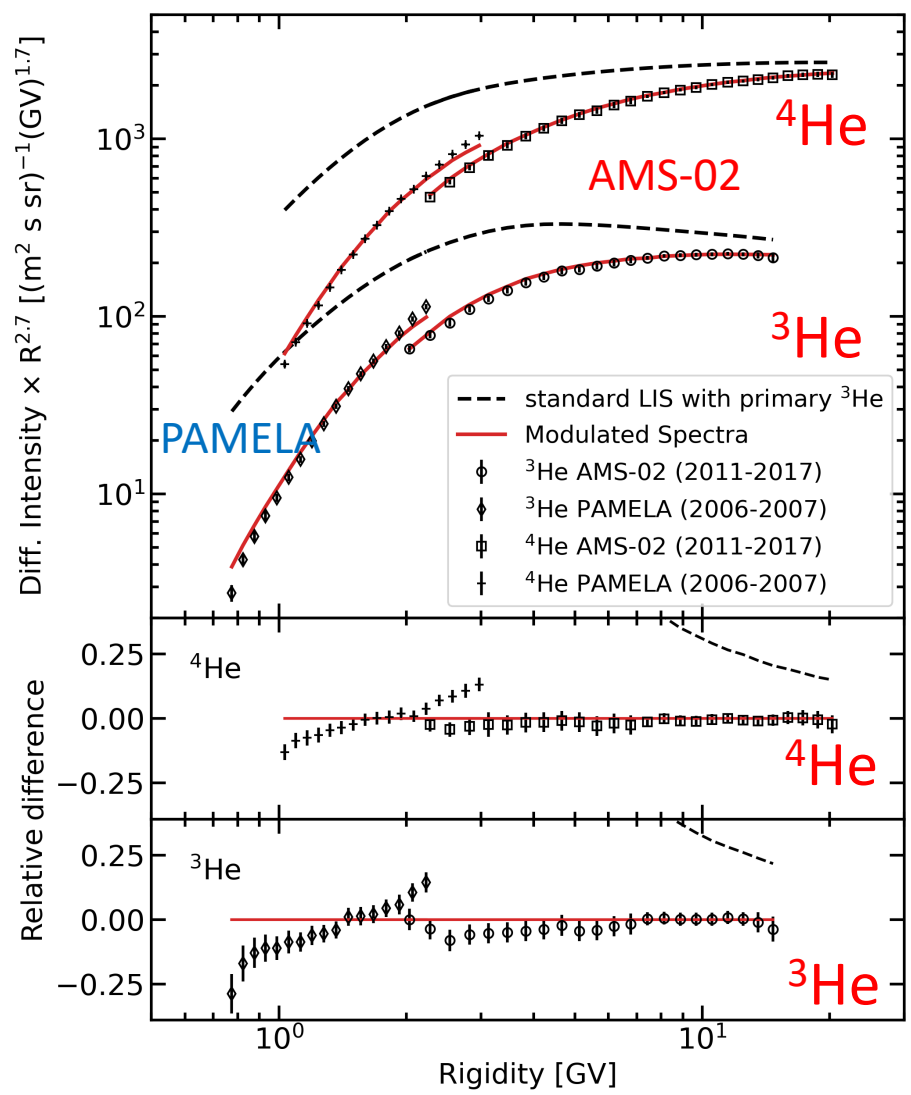


- Production near the CR source implies similar components in other secondaries (Li, Be, B) – not observed

^3He enrichment:

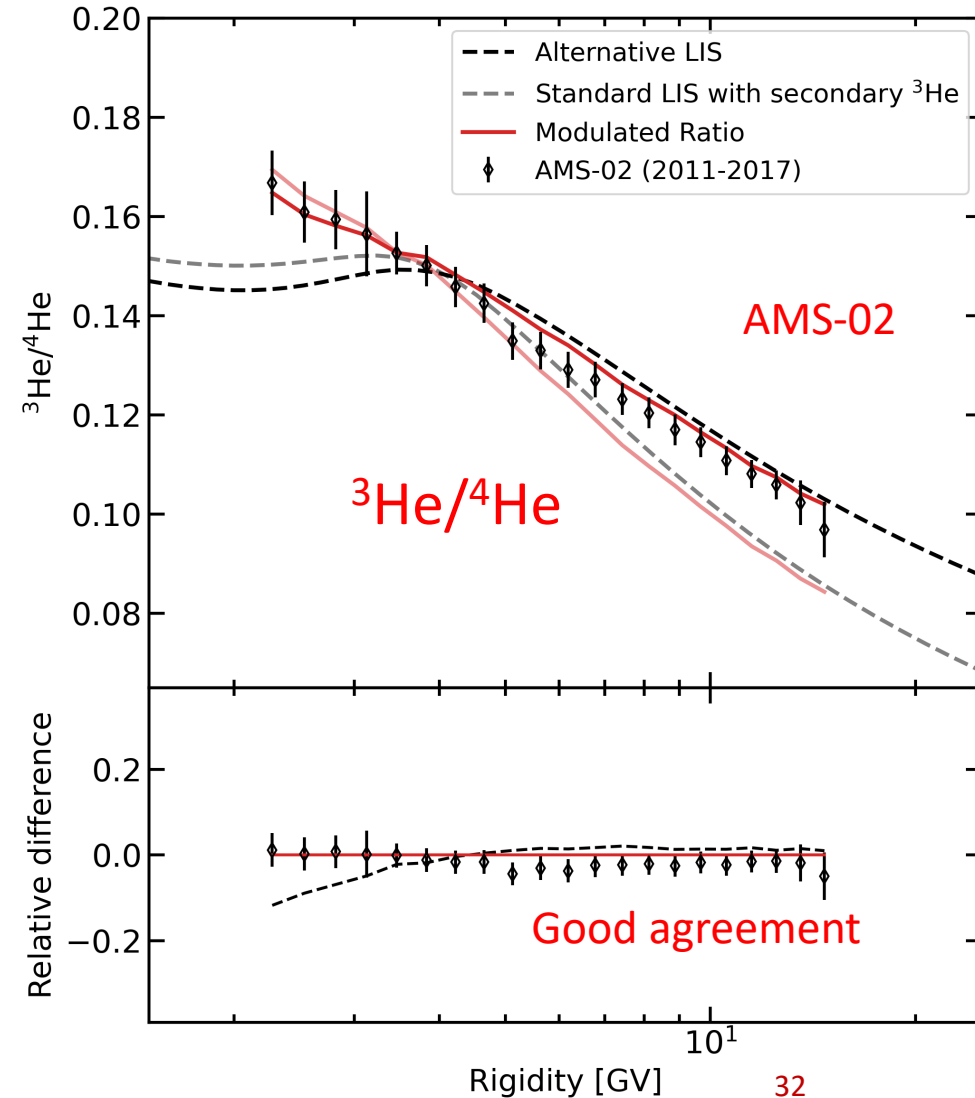
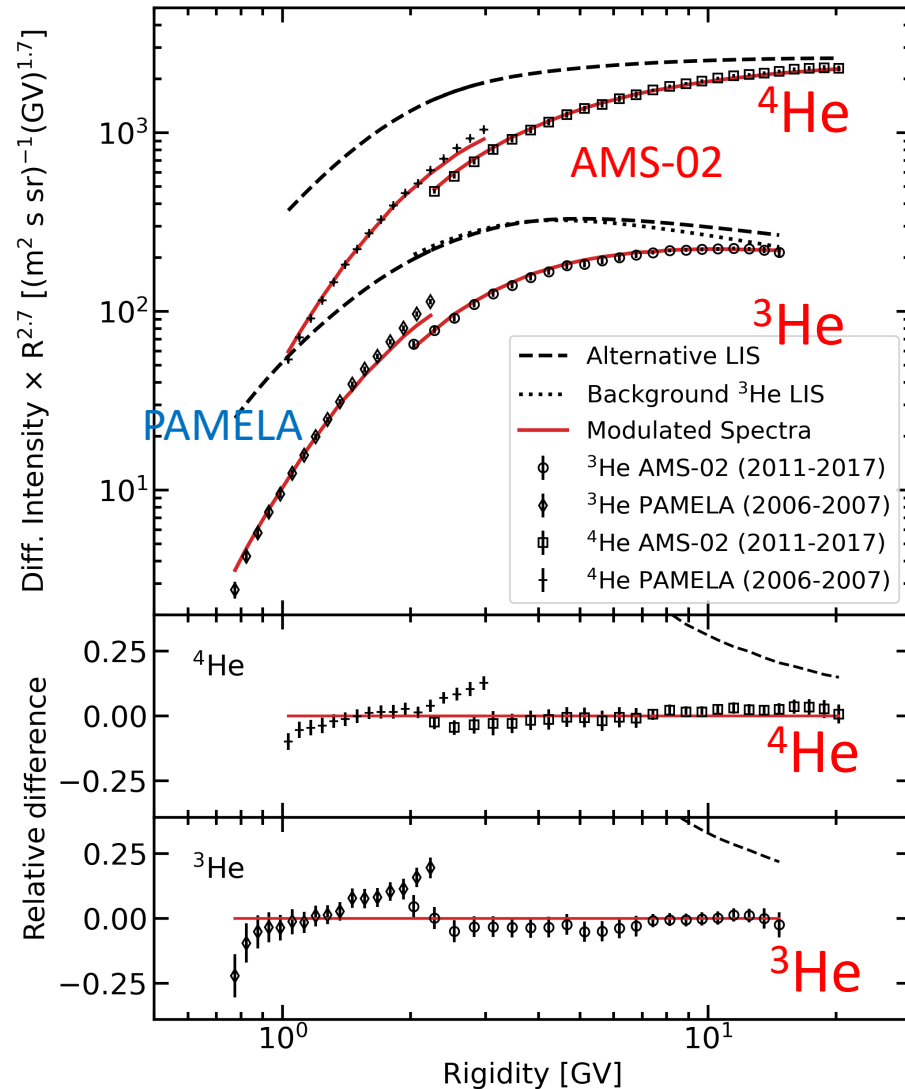
- Some SEP events exhibit resonant enhancements of $^3\text{He}/^4\text{He}$ up to 10,000-fold, which could even make ^3He dominant over H in rare events (Reames 2021)
- Even after ~50 yr of studies, the mechanism is unclear

II. Harder spectrum or primary ^3He



- Propagation is non-uniform. Can be tested with different sec/prim ratios
- Secondary ^3He production ($Z>2$) with standard propagation parameters (background)
- Then an MCMC scan with arbitrary ^4He abundance and all $Z>2$ abundances = 0 ($z_h=4$ kpc fixed)
- The final ^3He spectrum is the sum of two components

III. Alternative propagation $^3\text{He}/^4\text{He}$



Conclusion

- The excess in ^2H is probably the first direct evidence that chemical processes in the ISM, such as deuteration of organic molecules and dust grain surfaces, and ion sputtering may contribute to CR injection, and alter the CR source composition
- The excess in CR Boron, even though it is found at very low energies, is probably the most spectacular finding. It testifies that there might be primary Boron in CR sources and changes the way how we should derive the propagation parameters
- Beryllium seems to be truly secondary, and thus we should rely on the Be/O ratio rather than on the B/C or B/O ratio (Oxygen is truly primary)
- ^3He data can probe resonant acceleration OR the average diffusion coefficient over the large Galactic volume (larger than the B/C ratio)